A NECESSARY CONDITION AND A CORNER CONDITION FOR OPTIMAL COPLANAR ORBIT TRANSFER

by

Robert Dudley Culp

B.S., University of Oklahoma, 1960

M.S., University of Colorado, 1963

A thesis submitted to the Faculty of the Graduate School of the University of Colorado in partial fulfillment of the requirements for the degree of

Doctor of Philosophy

Department of Aerospace Engineering Sciences.

1966

This Thesis for the Doctor of Philosophy degree by

Robert Dudley Culp

has been approved for the

Department of

Aerospace Engineering Sciences

by

Adolf Busemann

Adolf Busemann

N. Vinh

N.X. Vinh

Date July 15, 1966

Culp, Robert Dudley (Ph.D., Aerospace Engineering Sciences)

A Necessary Condition and a Corner Condition

for Optimal Coplanar Orbit Transfer

Thesis directed by Professor Adolf Busemann

The problem considered is that of determining the means of orbit transfer in a Newtonian gravitational field which minimizes the characteristic velocity of the maneuver. The available thrust magnitude is assumed to be unlimited. The time duration of the maneuver is not considered. This restricts the analysis to the so-called time open problem, in which case only elliptical transfers between elliptical orbits need be considered. All motion is restricted to a plane. The sense of circulation in the orbit is not restricted.

This study is based on the approach proposed by Professor Adolf Busemann in the annual Ludwig Prandtl Memorial Lecture in Vienna, in April, 1965. This approach utilizes a configuration space of coplanar orbits which is particularly convenient for this problem. In this configuration space a metric body is constructed with which to measure the relative displacement of an orbit caused by infinitesimal impulses applied at all positions of the orbit and

in every direction in the plane. This metric body is analyzed to obtain properties of the minimal paths of this space. The infinitesimal impulses can be used to construct either finite impulses or continuous thrust maneuvers.

This analysis yields a necessary condition which must be satisfied in order that a maneuver be optimal. In addition, this study produces a corner condition which must be satisfied at the junction of two maneuvers in order that the entire maneuver be optimal. It is shown that optimal maneuvers are nearly always composed of finite impulses. Continuous thrust optimals are very rare special cases and are treated only briefly. A method is given for generating multiple impulse trajectories which satisfy both the necessary condition and the corner condition, and an example of such construction is displayed. The analysis is completed numerically and the results are presented graphically.

This abstract is approved as to form and content. I recommend its publication.

Signed Adolf Busemann
Faculty member in charge of dissertation

TABLE OF CONTENTS

LIST OF FIGURES

I. INTRODUCTION

a) The Basic Problem

In the aerospace engineering sciences there is an important problem of basic orbital transfer which, even with the obvious simplifications and strong current interest, has only been partially investigated. In general, this problem is that of transferring a space vehicle, which is in orbit about a gravitational body, from its given orbit to a second orbit and performing the transfer in some optimum sense. The model which suggests itself is an attractive central force field with the magnitude of the force inversely proportional to the square of the distance from the center of attraction. This is the well-known Newtonian, or inverse square, gravitational field.

The criterion of optimization logically might be minimization of fuel expenditure, since in a simple model of the space vehicle fuel expenditure provides a direct measure of the cost of a maneuver in terms of weight or bulk. A characteristic velocity can be defined which furnishes a direct measure of fuel expenditure in terms of a theoretical maximum achievable velocity change for a given expenditure of propellent. For a simple rocket traveling in a straight line in the absence of any external force, the differential expression for the change of velocity effected by the use of a differential amount of propellent, dm, is

$$dv = - \frac{dm}{m} \cdot c \qquad (1)$$

where m is the instantaneous mass of the rocket and unexpended fuel, and c is the instantaneous exhaust velocity of the propellent.

The characteristic, or latent, velocity may thus be defined as

$$\varphi \equiv \int_{m}^{m_o} \frac{c}{m}\, dm = \int_{t_o}^{t} \tau\, dt \qquad (2)$$

where τ is the instantaneous magnitude of the acceleration due to thrust.

If the thrust magnitude is unlimited then the velocity change can be assumed to take place discontinuously, and the characteristic velocity becomes, as expected, the magnitude of the impulsive velocity change.

The problem thus stated is of classical merit, having been treated as early as 1925 by Hohmann.[1] The problem is that of determining the means of orbital transfer in a Newtonian gravitational field which minimizes the characteristic velocity.

b) Restrictions and Assumptions

It is assumed here that the available thrust magnitude is unlimited. As is shown in this study the practical result of this assumption is the emergence of finite impulsive velocity changes as the optimal maneuvers in nearly all cases. This is not unexpected. It has been shown by Contensou[4], Lawden[5], and several others[6,7] that the requirements for an optimal trajectory using less than maximum thrust are so stringent as to render such solutions unrealistic. With the thrust unlimited the analysis can be carried out using infinitesimal impulses to construct both finite impulses and continuous thrust maneuvers. Thus, when the thrust is unlimited only impulsive velocity changes need be considered in order to determine the optimal trajectories, be they impulsive or continuous thrust. Even in the case where an upper limit is placed on the thrust magnitude, knowledge of the optimal unlimited thrust maneuvers provides a powerful tool for finding the restricted thrust optimal trajectories[8,9,19].

It is assumed that time is eliminated from the problem. Then only this so-called time open problem is considered. The results of this assumption are far-reaching. Basically, this assumption eliminates any necessity for considering hyperbolic trajectories either as initial or final trajectories, or as arcs of a minimum fuel trajectory between given trajectories. Time open transfer between

two trajectories of an escape nature (either hyperbolic or parabolic trajectories) can always be effected using only infinitesimal impulses, and time open transfer between an elliptical orbit and either an hyperbolic or a parabolic orbit can be accomplished by an impulse equal to the minimum impulse required for escape from the elliptical orbit.[10] Further, Marchal[11] has shown that in the time open case an hyperbolic arc cannot form part of an optimal trajectory.

Thus, the time open transfer problem admits only elliptical transfer between elliptical orbits as an area of interest. Between any two elliptical orbits there is the upper bound on characteristic velocity requirements provided by the competition in the large from the four impulse maneuver with a characteristic velocity equal to the sum of the minimum impulses required for escape from the two orbits[10,11]. This provides an easy comparison test for all proposed maneuvers in this problem.

Finally, it is assumed here that all motion takes place in a plane passing through the center of attraction. This restriction to coplanar orbits reduces the number of degrees of freedom of the orbits from five to three.

c) The Configuration Space

With the restrictions thus placed on this study, the objectives sought are the minimum characteristic velocity, impulsive, coplanar, elliptical, time open maneuvers in a Newtonian gravitational field. In a Newtonian gravitational field the trajectories are Keplerian. That is, the trajectories are conic sections. It will be advantageous to construct a configuration space which preserves, and even enhances, this property of the trajectories. This configuration space was introduced by Professor Adolf Busemann in the annual Ludwig Prandtl Memorial Lecture in Vienna, in April, 1965[2].

This configuration space of coplanar elliptical orbits is defined in the following manner. It was previously noted that there are three degrees of freedom for these coplanar orbits. Therefore, the space will be three dimensional. All of the ellipses have one common focus, the center of attraction. The origin of the orbit space is taken as this common focus. In the plane of the orbits orthogonal axes are taken along which are measured the coordinates of the second focus of every ellipse. Thus, two of the coordinates of the configuration space are given by the vector from the common focus to the second focus of the ellipse, sometimes called the vacant focus. This is a two vector lying in the plane of the orbits. A right-hand orthogonal system is formed by taking as a third coordinate normal to the plane of the orbits the length of the major

axis of the ellipse, ℓ.

The major axis of an ellipse must be at least as long as the distance between its foci. Therefore, this configuration space of coplanar elliptical orbits is confined by the cone of revolution about the ℓ axis with semivertex angle 45°, in which $\ell \geq f$. This cone is labelled Σ (Figure 1.). Points on the cone Σ correspond to degenerate ellipses with $\ell = f$ and a minor axis of zero length. Points on the ℓ axis correspond to circles. Since the eccentricity e is given by f/ℓ, an ellipse of eccentricity e must lie on a cone of revolution about the ℓ axis with semivertex angle $\tan^{-1} e$. That is, the larger the angle OE makes with the ℓ axis, the larger is the eccentricity of ellipse E.

In order to obtain other useful properties of this orbit space and to become more familiar with the relations among ellipses under this representation, one should note that if two ellipses intersect then the following inequality must hold.

$$\left| (\ell' - r) - (\ell - r) \right| \leq \left| \overline{f'} - \overline{f} \right|$$

or (3)

$$\left| \ell' - \ell \right| \leq \left| \overline{f'} - \overline{f} \right|$$

This is obvious from Figure 2. The existence of the triangle formed by the point of intersection and the two second foci of the ellipses provides this inequality. If the two ellipses are tangent at a point, then the two flight path angles, γ and γ', are equal and the

triangle degenerates to a straight line. Thus, the equality in (3) holds in the case of tangency.

Then the equality in (3) states that if any ellipse E' is tangent to a given ellipse E, then in this configuration space E' must lie on the surface of the cone of revolution with axis parallel to the ℓ axis, semivertex angle of 45°, and vertex at the point E. The inequality in (3) states that a point representing an intersecting ellipse must lie outside this cone. It follows that points interior to the cone represent ellipses which do not intersect E. Since those points inside the upper half cone (above the point E) have major axes longer than that of E, these ellipses lie wholly outside E. Similarly, points inside the lower half cone represent ellipses wholly contained inside the ellipse E.

Therefore, in this configuration space of coplanar elliptical orbits every orbit has an associated cone which neatly divides the remaining ellipses of the space into accessible and inaccessible orbits. Those orbits which intersect or are tangent to the original orbit are immediately accessible via impulsive velocity change without recourse to an intermediate orbit. Those orbits which do not touch the original orbit are inaccessible in the sense that an intermediate orbit is necessary in order to reach them, (Figure 3).

From the construction of this space it is apparent that the plane of the second focus vectors is identical to the physical plane of the orbit. The orbit may be drawn on this plane to

further aid in visualization of certain features of the space. Physical constructions in the orbital plane and representations in the three dimensional configuration space may be completely interwoven. In particular, this feature is useful in determining the set of all ellipses in the plane which pass through a given point in space. For a point P of the physical plane, it is evident that the ellipse passing through P which has the shortest major axis is the degenerate ellipse with second focus at P, and ℓ equal to f. It is also apparent that any ellipse passes through P if and only if it is tangent at P to this degenerate ellipse. From the previous discussion, all ellipses tangent to a given ellipse are represented in this configuration space by the points lying on the associated cone of the given ellipse. Points on the upper half of the associated cone are ellipses which are externally tangent to the given ellipse.

The conclusion is that in this configuration space the locus of ellipses which pass through a given point P in the physical plane is the upper half of the associated cone of the degenerate ellipse with second focus at P (Figure 4).

This result may also be established in the following manner. For an otherwise arbitrary elliptical orbit E which passes through the point P, the distance from its second focus F to P is $\ell - r$, where r is the distance of P from the origin. On the verticals rising from P and F the points D and G are at a distance r

from the physical plane (Figure 5). The point E, of course, is a distance ℓ above F. Then DG is of length $\ell - r$, as is EG. The line DG is perpendicular to both verticals. Therefore, DE makes an angle of 45° with the extension of PD. Since the ellipse E was arbitrary aside from its passing through P, it follows that any ellipse which passes through P must be represented in the configuration space on the upper half cone of revolution with vertex a distance r above P, semivertex angle of 45°, and axis of revolution the vertical rising from P. This cone is just the associated cone of the degenerate ellipse with second focus at P. This is precisely the result obtained above.

This property leads immediately to another useful property of the configuration space. The point E representing the ellipse in configuration space must lie on every half cone representing all ellipses passing through a point of the ellipse E. This shows that the intersection of the associated cone of E with the configuration space boundary cone Σ projects on the physical plane as the physical orbit E. Another way of looking at this is by noting that at any point of the ellipse E, the degenerate ellipse with second focus at that point is tangent to the original orbit. Therefore, the points in the configuration space representing these degenerate ellipses lie both on the associated cone of E and the boundary cone Σ. This confirms the previous statement.

A discussion of the properties of this configuration space, the powerful visualization of orbital problems which it provides, the advantages of the fact that in this space orbital problems remain problems of conics, and the use of this configuration space in approaching a specific problem can be found in reference 12.

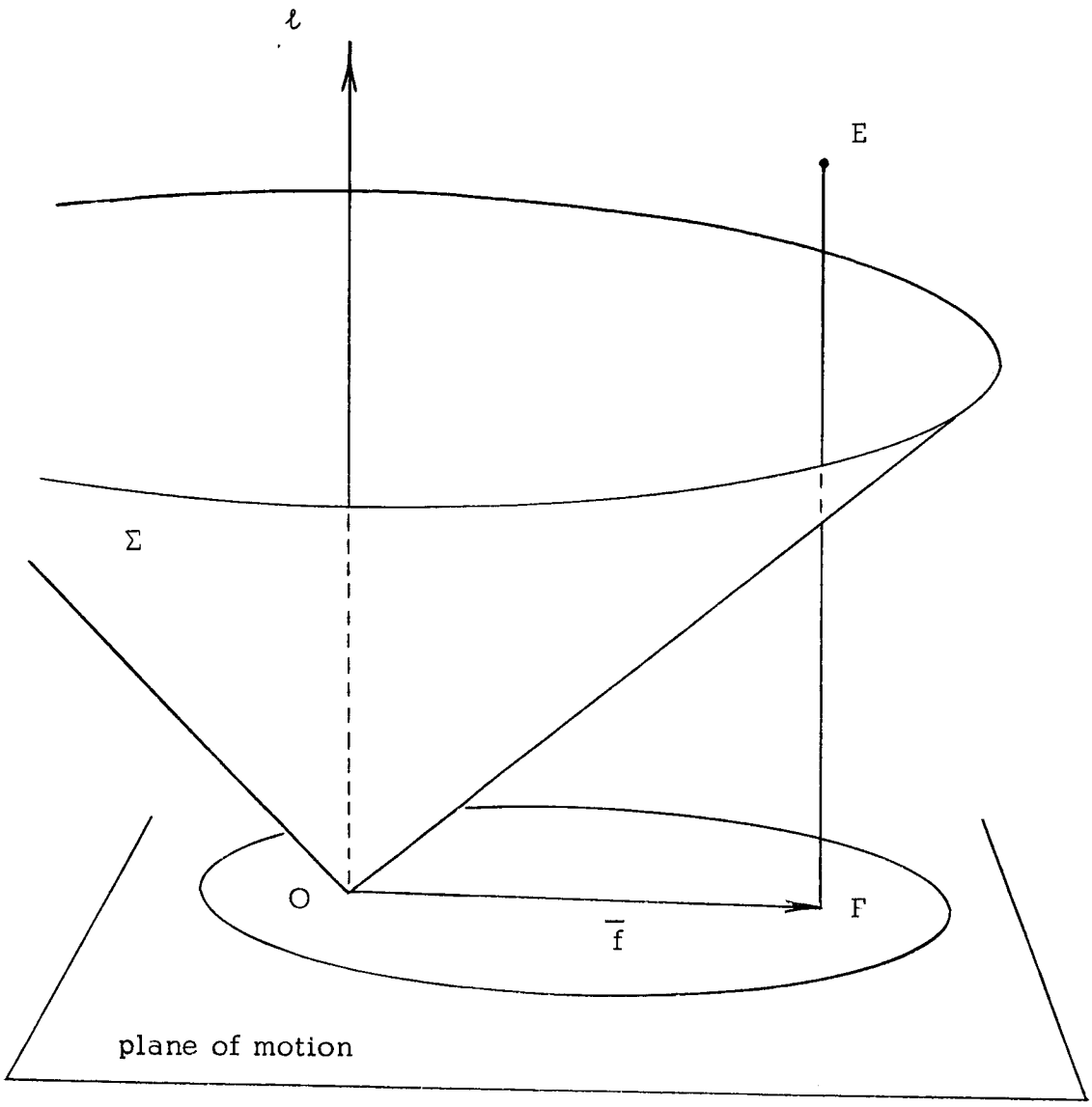

Figure 1. Busemann's configuration space of coplanar orbits.

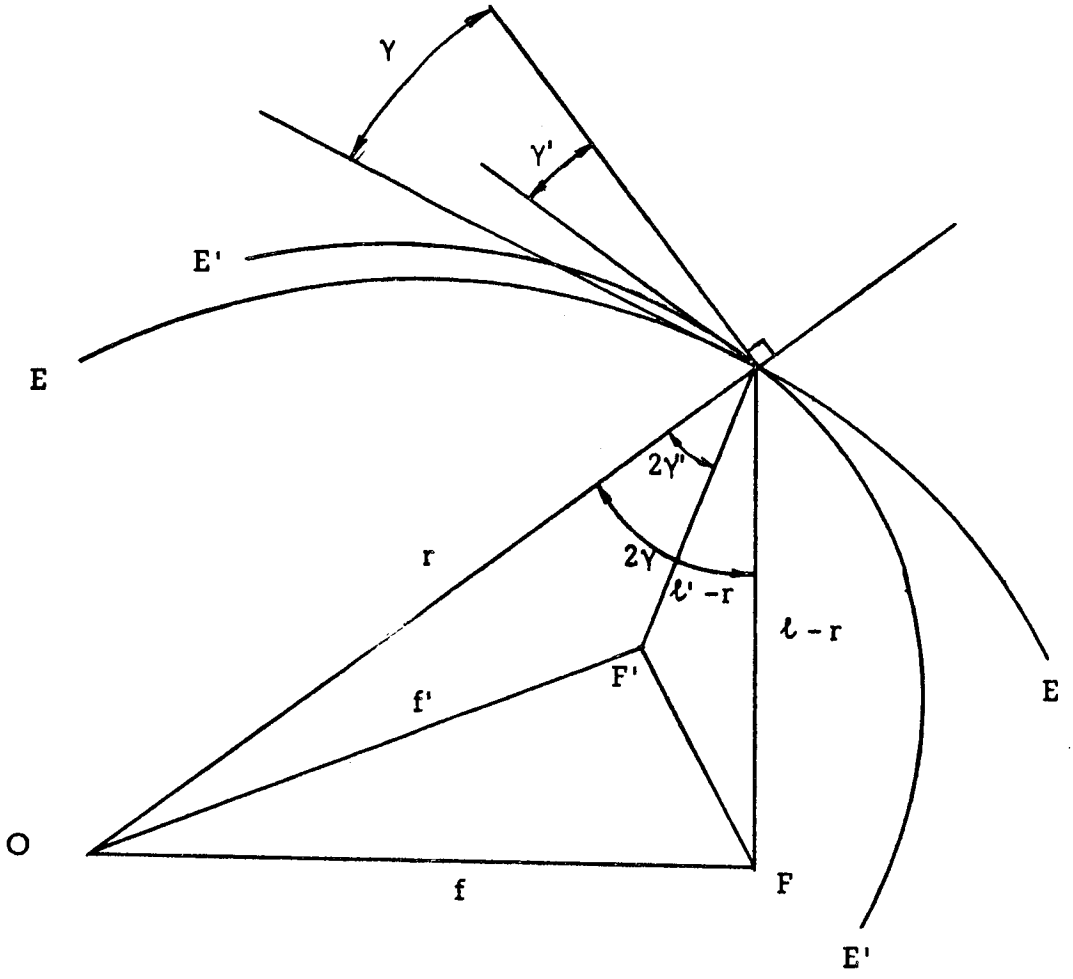

Figure 2. Intersection of two orbits, drawn in the physical plane.

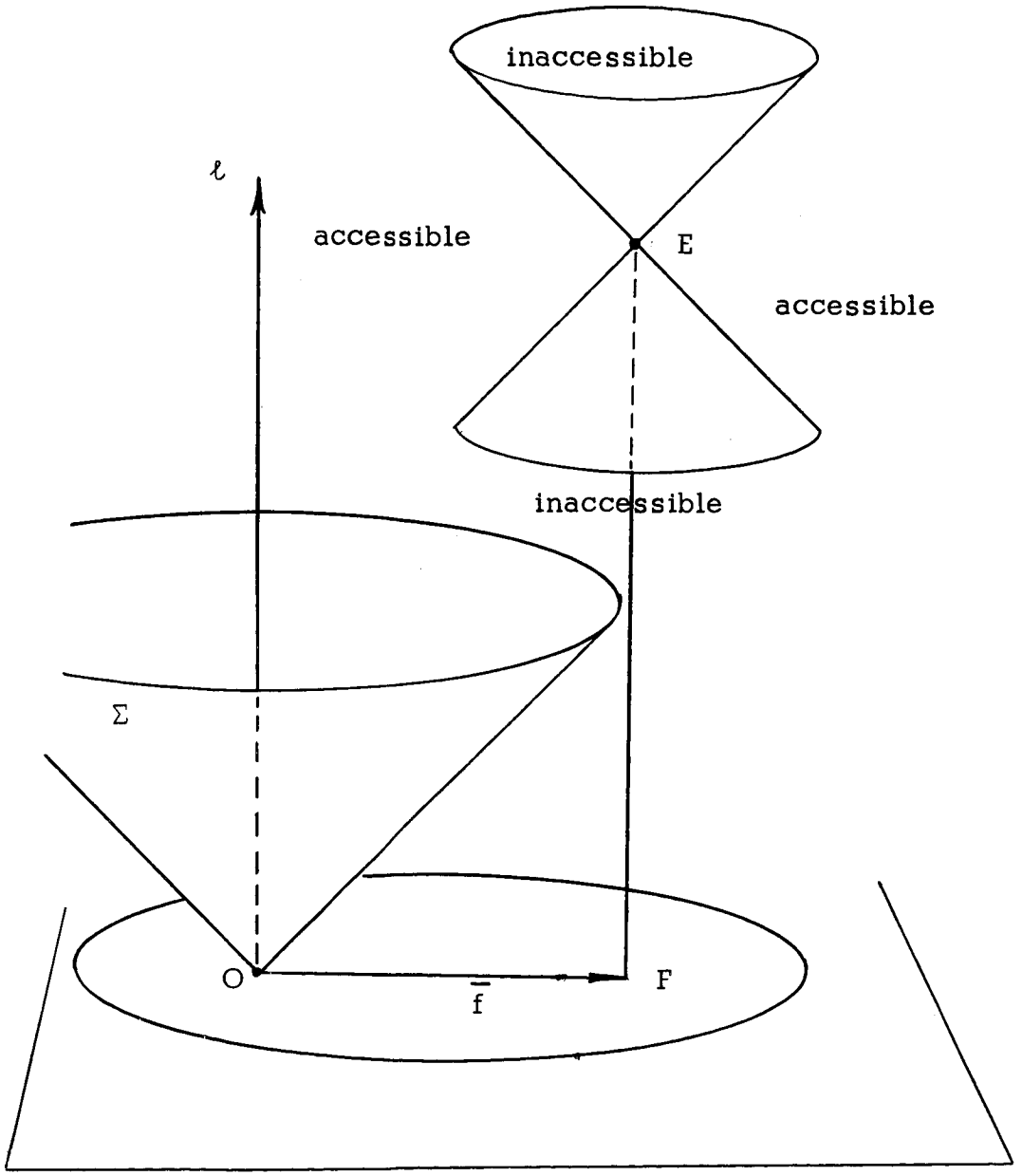

Figure 3. The associated cone of an orbit dividing the configuration space into accessible and inaccessible regions.

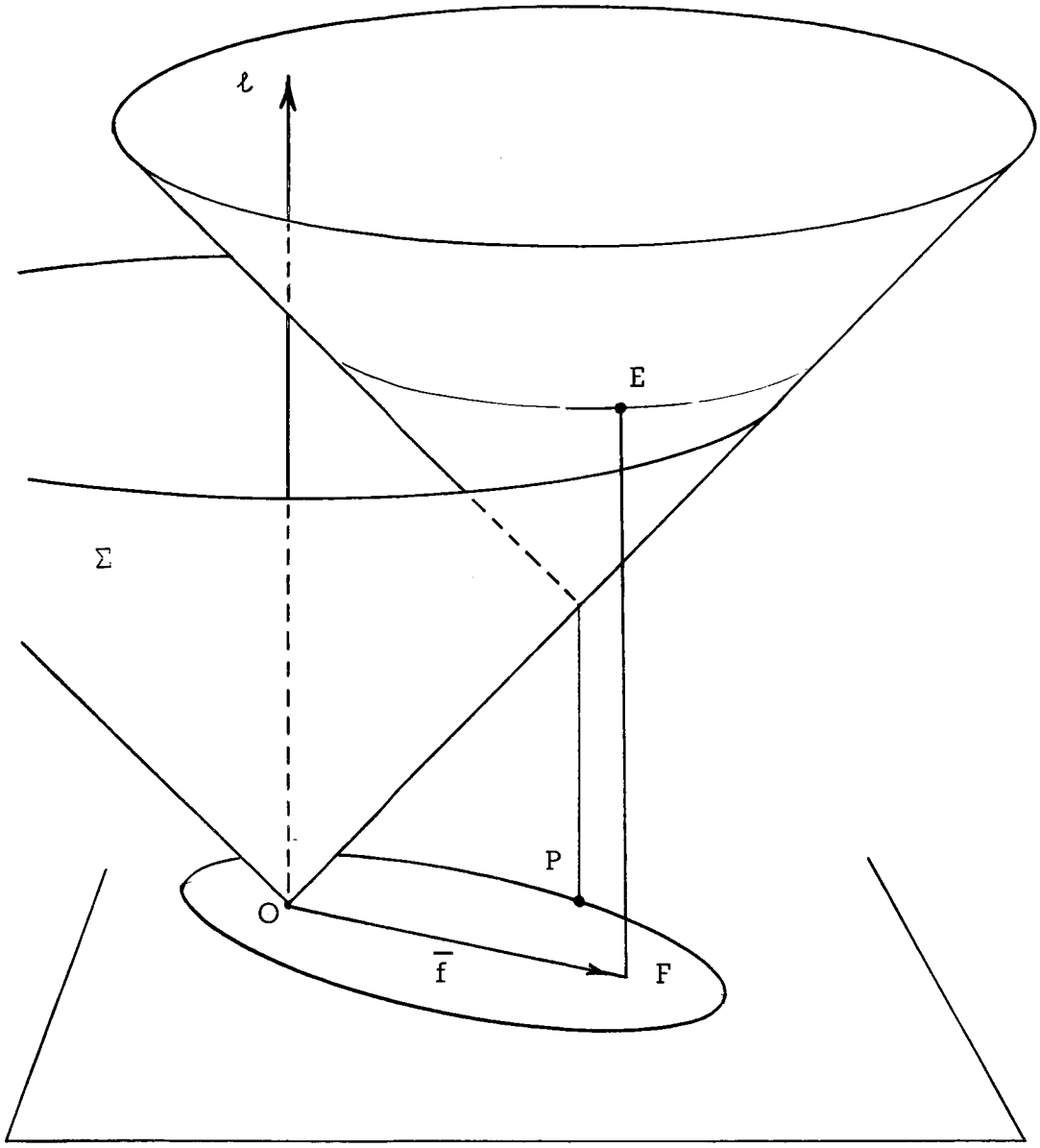

Figure 4. The locus in configuration space of orbits through a given point P.

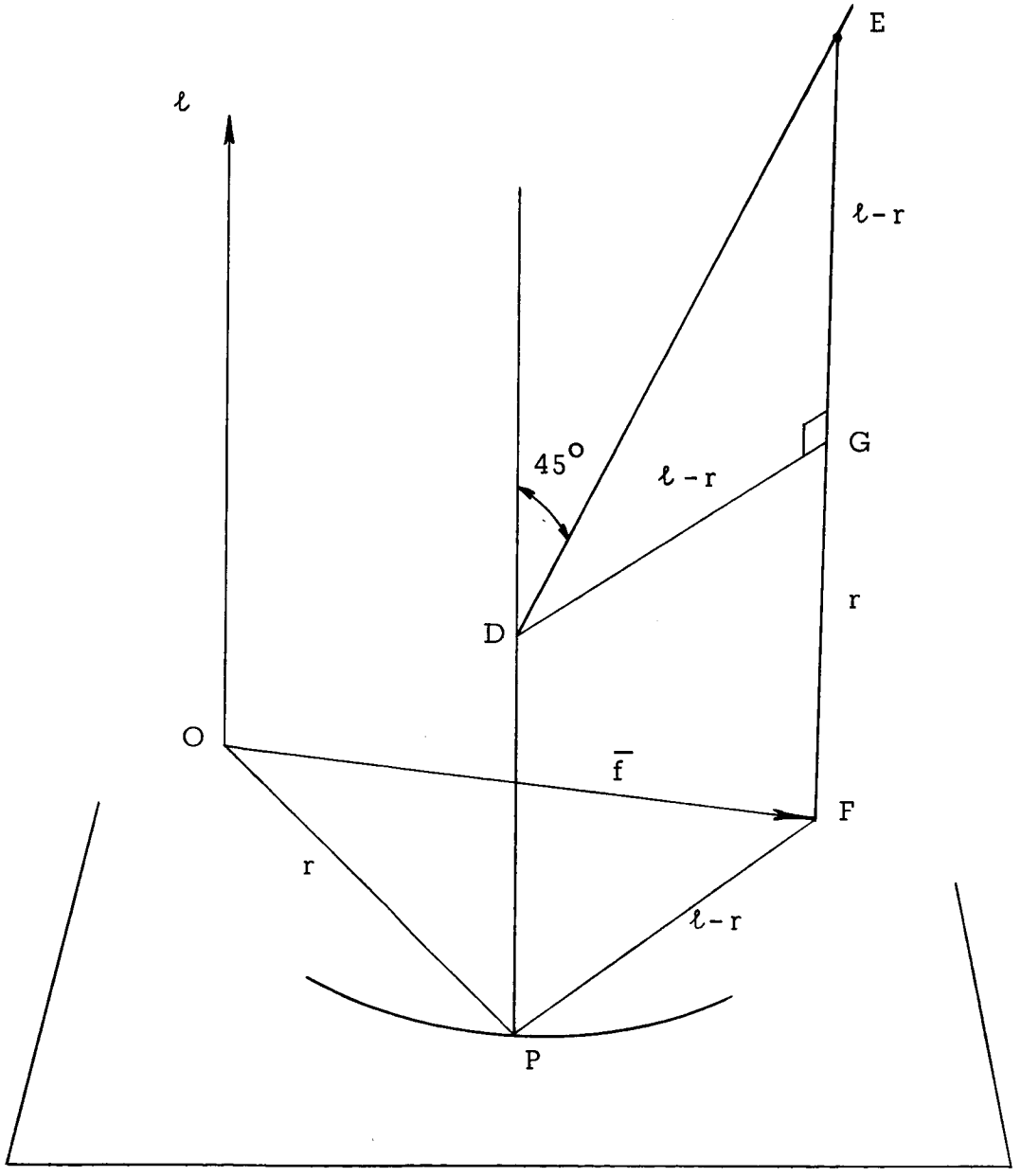

Figure 5. Element relations for an orbit through a given point P.

II. THEORY AND PROCEDURE

a) General Approach

The problem under consideration is the time open problem of coplanar orbital transfer by impulsive velocity change. The property of the maneuver to be optimized is the characteristic velocity. In the case of a single impulsive velocity change the characteristic velocity is simply the magnitude of the velocity change vector.

The analysis which is used in this study results in the establishment of a necessary condition which must be satisfied by a proposed impulsive maneuver in order that it be an optimal maneuver. Also obtained is a corner condition which must be satisfied when two impulses are joined if the resulting multiple impulse maneuver is to be optimal. The approach used here is that set forth by Professor Busemann in his Prandtl lecture[2].

The basic idea is to consider the variation in the orbital parameters caused by an infinitesimal impulsive velocity change of magnitude dv. Since the problem is time open no preference is given to any position on the original orbit. At every position around the orbit the effect of applying the impulse dv in every direction of the plane is considered. In the configuration space the result is a surface of orbits which are attainable from the original orbit through an impulsive change of velocity of magnitude dv. This surface forms a body in the three dimensional

configuration space which will be referred to as the metric body of the space. It provides a local measure of the relative effectiveness of all the available maneuvers which are admissable under the assumptions made.

This metric body is a continuous function of the initial ellipse. Therefore, for initial ellipses restricted to a sufficiently small neighborhood of a given ellipse the metric body will be in every respect as nearly identical as desired to the metric body of the given ellipse. Thus, only those portions of the metric body which are convex can possibly be optimal. Any maneuver which ends with an orbit represented by a point on a concave portion of the metric body can be replaced by a linear combination of two maneuvers from the convex portions of the body with a total characteristic velocity smaller than that of the original maneuver (Figure 6).

In this manner the original metric body is replaced by an improved metric body consisting of the convex portions of the original metric body but with the concave portions covered by a developable surface. This developable surface is formed by the bitangential lines between sets of two points of the body so situated that the bitangent is completely outside the body. This follows from the meaning of convex and concave portions of the body. A body is convex in case it wholly contains the straight

line joining any two of its points. The metric body is rendered convex by including in it all points lying on the straight line joining any two points of the original metric body. Only those points on the surface of the improved metric body represent possibly optimal maneuvers. This construction is equivalent to the construction by bitangential lines mentioned first. The bitangential line construction breaks down where the original metric body does not have a well-defined tangent plane. Then the second, more basic construction must be used. It will be seen that for this problem these exceptional cases can be handled quite simply.

The resulting body is entirely convex. Thus, the surface of this improved metric body represents the maximum local progress in any direction in configuration space which can be achieved from a given orbit through the use of a fixed infinitesimal amount of characteristic velocity, dv. For this optimum use only certain maneuvers are allowed. These are those maneuvers represented by points on the surface of the improved metric body which are also points on the surface of the original metric body. Points which are on the surfaces of both the improved metric body and the original metric body will be said to form the convex portion of the metric body. Therefore, the necessary condition for optimal coplanar orbital transfer which is obtained through this analysis is that a

maneuver must be represented throughout by points on the convex portion of the local metric body of the configuration space.

An alternative way of stating this can be found by observing that a coplanar impulsive maneuver is represented in the configuration space by an arc. This is evident since the instantaneous velocity vector and position vector completely determine the elliptical orbit of the vehicle. During the impulse, the position is constant and the velocity varies continuously. Therefore, the point representing the orbit as the impulse is applied describes an arc in configuration space. The arc in configuration space representing a continuous thrust maneuver is made by joining the arcs of the infinitesimal impulses which form it. That is, the arc of a continuous thrust, or intermediate thrust maneuver is generated by the continuous variation of the velocity vector and the position in the plane.

In this light, the necessary condition of this study can be stated as follows. A necessary condition for an optimal coplanar orbital maneuver is that in this configuration space the arc representing this maneuver must always pierce the metric body through its convex portions as this metric body moves along the arc.

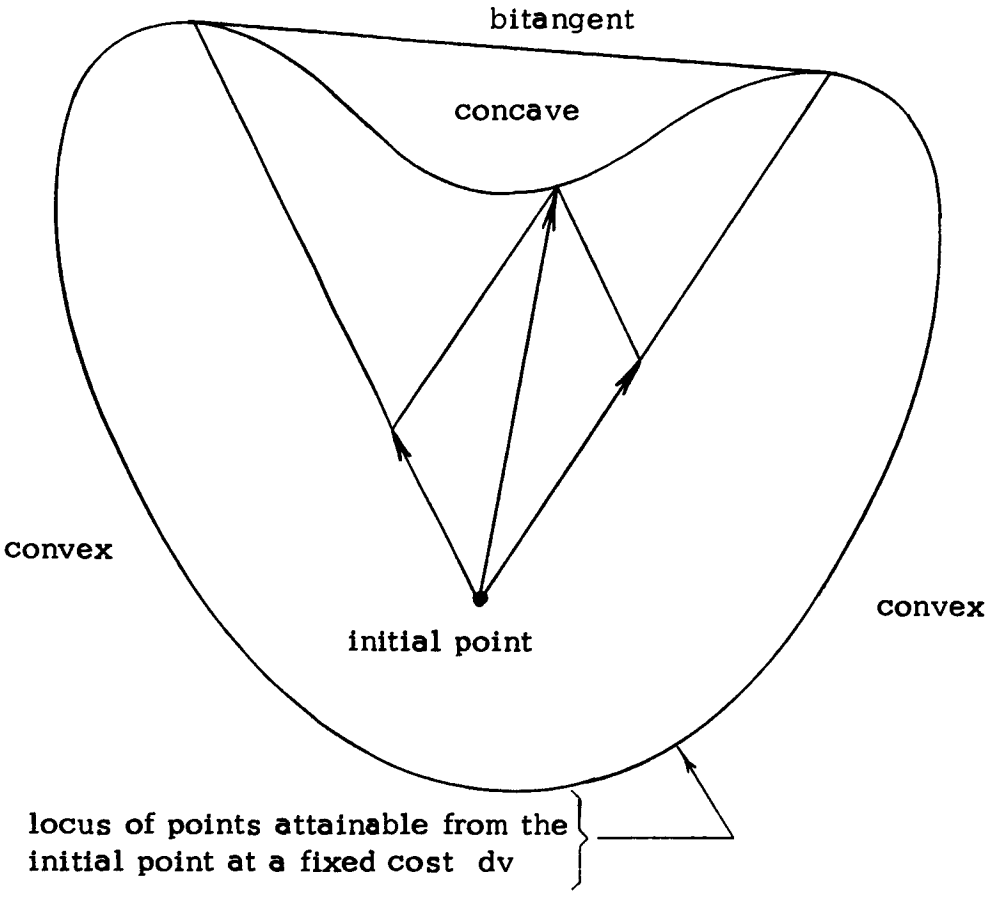

Figure 6. An arbitrary metric body showing the concave portion replaced by an external bitangent.

b) The Metric Body

The application of the impulse dv is controlled by two variables. One specifies the position on the original orbit at which the impulse is applied, the other specifies the direction of the impulse, subject to the restriction that the impulse must be in the plane of motion. It is convenient for computational reasons to use the intrinsic parameters of the problem for this purpose. Used for specifying the position on the ellipse is the angle δ between the line from the second focus F to the common focus O, and the line from F to the position P on the ellipse (Figure 7). The angle is measured positive from periapsis in the direction of the velocity. The velocity around the orbit is assumed to be in a right-hand sense about the ℓ axis. The direction of the impulse is measured by the angle ψ between the velocity vector and the impulse vector, measured positive from the velocity vector outward away from the orbit.

For a particular impulse with given δ and ψ, the resulting point on the metric body may be found by considering the movement of the second focus F caused by the impulse. From the energy integral

$$v^2 = 2\mu\left[\frac{1}{r} - \frac{1}{\ell}\right] \qquad (4)$$

comes

$$\ell = \frac{r}{1 - \frac{v^2 r}{2\mu}} \tag{5}$$

Since ℓ is affected by only the tangential velocity increment, dv cos ψ, the change in ℓ is given by

$$d\ell = \frac{vr^2}{\mu\left[1 - \frac{v^2 r}{2\mu}\right]^2} \, dv \cos \psi \tag{6}$$

Using (4) one obtains

$$d\ell = \frac{v\ell^2}{\mu} \, dv \cos \psi \tag{7}$$

This is the magnitude of the component of $\overline{df}$ parallel to PF.

$$|\overline{df}| \cos \psi = d\ell \tag{8}$$

The velocity increment normal to the flight path, dv sin ψ, does not affect ℓ since it does not change the energy of the orbit. It simply rotates the position of F on a circle of radius $\ell - r$ centered at the vehicle position in the orbit. The angle of rotation is twice the change in the flight path angle, $d\gamma$. Therefore, the magnitude of the vector change in $\overline{f}$ perpendicular to PF is given by

$$|\overline{df}| \sin \psi = 2d\gamma\,(\ell - r) \tag{9}$$

Using

$$d\gamma = \frac{dv}{v} \sin \psi \tag{10}$$

and again resorting to (4), one may write

$$|\overline{df}| \sin \psi = \frac{\frac{v\ell^2}{\mu} dv \sin \psi}{1 + \frac{v^2 \ell}{2\mu}} \tag{11}$$

or

$$|\overline{df}| \sin \psi = \frac{v\ell}{\mu r} dv \sin \psi$$

The locus of $\overline{f}$ as ψ varies from 0 to 2π, and thus as the impulse $\overline{dv}$ makes a full circle, is the ellipse centered at F

$$\frac{(d\ell)^2}{\left[\frac{v\ell^2}{\mu} dv\right]^2} + \frac{[2d\gamma(\ell - r)]^2}{\left[\frac{v\ell}{\mu r} dv\right]^2} = 1 \tag{12}$$

For a new coordinate system based on these changes in the second focus of the ellipse, it is convenient to define

$$\begin{aligned} \xi &\equiv |\overline{df}| \cos \psi \\ \eta &\equiv |\overline{df}| \sin \psi \end{aligned} \tag{13}$$

Then equation (12) may be written

$$\frac{\xi^2}{\left[\frac{v\ell^2}{\mu} dv\right]^2} + \frac{\eta^2}{\left[\frac{v\ell}{\mu r} dv\right]^2} = 1 \tag{14}$$

The orientation of this ellipse is given by the angle δ. By

the law of cosines (Figure 7) the following holds.

$$\cos\delta = \frac{1}{2}\left[\frac{f}{\ell} + \frac{\ell}{f}\right] - \frac{\mu}{v^2\ell}\left[\frac{\ell}{f} - \frac{f}{\ell}\right] \qquad (15)$$

From (15) comes

$$\frac{v^2\ell}{2\mu} = \frac{\ell^2 - f^2}{(\ell^2 + f^2) - 2f\ell\cos\delta} \qquad (16)$$

which leads to

$$\frac{v\ell^2}{\mu^{1/2}} = \left[\frac{2\ell^3(\ell^2 - f^2)}{\ell^2 + f^2 - 2f\ell\cos\delta}\right]^{1/2} . \qquad (17)$$

Substituting (17) into the equations (7) and (11) and using (8) and the new coordinates (13), one obtains the coordinates ξ and η of points on the metric body generated at one position of the given orbit. In terms of the intrinsic parameters ψ and δ these coordinates are

$$\xi = \frac{dv}{\mu^{1/2}}\left[\frac{2\ell^3(\ell^2 - f^2)}{\ell^2 + f^2 - 2f\ell\cos\delta}\right]^{1/2}\cos\psi$$

$$\eta = \frac{dv}{\mu^{1/2}}\,\frac{[2\ell^3(\ell^2 - f^2)]^{1/2}[\ell^2 + f^2 - 2f\ell\cos\delta]^{1/2}}{2(\ell^2 - f\ell\cos\delta)}\sin\psi \qquad (18)$$

A more frequently used notation is that of replacing f by the eccentricity e, given by f/ℓ. In terms of e (18) is

$$\xi = \frac{dv}{\mu^{1/2}}\left[\frac{2\ell^3(1 - e^2)}{1 + e^2 - 2e\cos\delta}\right]^{1/2}\cos\psi \qquad (19)$$

$$\eta = \frac{dv}{\mu^{1/2}} \frac{[2\ell^3(1 - e^2)]^{1/2} [1 + e^2 - 2e \cos \delta]^{1/2}}{2(1 - e \cos \delta)} \sin \psi \tag{19}$$

Since the change in the ξ direction is seen to be the change in the length of the major axis from equations (8) and (13), the vertical displacement of the point E in configuration space will be equal to ξ. Therefore, this ellipse representing the points of the metric body generated at one position on a given orbit will appear in configuration space with its plane tilted at 45° to the physical plane. Because its major axis is generated by forward and rearward tangential thrusts, this major axis will coincide with a generator of the associated cone of E (Figure 8).

An ellipse on the metric body is produced for every different value of δ. If the original orbit is circular, e equal to zero, then all of the ellipses are identical, and the metric body is produced by rotating an ellipse about an axis through its center at an angle of 45°. This metric body and the improved metric body which has been made convex by a developable surface are shown in Figure 9. In this case of a circular original orbit the only unforbidden maneuvers are tangential imulses represented by the rims of the can-shaped improved metric.

If the original orbit is elliptical, then the size and shape of the ellipses which make up the metric body vary as δ varies.

Figures 10 and 11 serve to illustrate the general character of this metric body. The dotted line in Figure 10 and the solid inner line in Figure 11 show where the ends of the major axes of these ellipses lie on the associated cone. These are the points generated by tangential maneuvers. It is apparent that, except at the apses with δ equal to 0 or 180°, the metric body rises upward and outward from these tangential points. Thus, these points lie in a concave portion of the metric body and cannot represent optimal maneuvers. This agrees with the fact which has been shown previously[13,14] that in general the cotangential orbit transfer is nonoptimal. This result is stronger in that it shows that, except where the velocity vector is horizontal, no tangential maneuver can be optimal, not even a single impulse transfer.

The improved metric body made by covering the metric body with a developable surface is shown in Figure 12. Only the narrow edges around the top and bottom remain from the original metric body. The points on these lips represent maneuvers which satisfy the necessary condition for an optimal maneuver. At the apses of an elliptical orbit and all around a circular orbit the only maneuvers which satisfy this condition are the tangential impulses. That is, when the velocity vector is horizontal the only possible optimal maneuvers are tangential maneuvers. This agrees with the previously established result that the Hohmann type of maneuver

is an absolute optimum[15,16].

Figure 12 shows that there are three separate developable surfaces which cover concave portions of the metric body. There is the side surface, or mantle, which wraps around the body covering most of the accessible directions in configuration space, and there are top and bottom surfaces which completely cover the inaccessible directions inside the associated cone. The only convex portions of the original metric body are those lips which emerge between these developable surfaces. It is evident that these represent impulses which are nearer tangential than normal to the velocity vector. The boundaries of these lips will be calculated in the following sections of this analysis in order to provide the desired necessary condition for optimal orbit transfer.

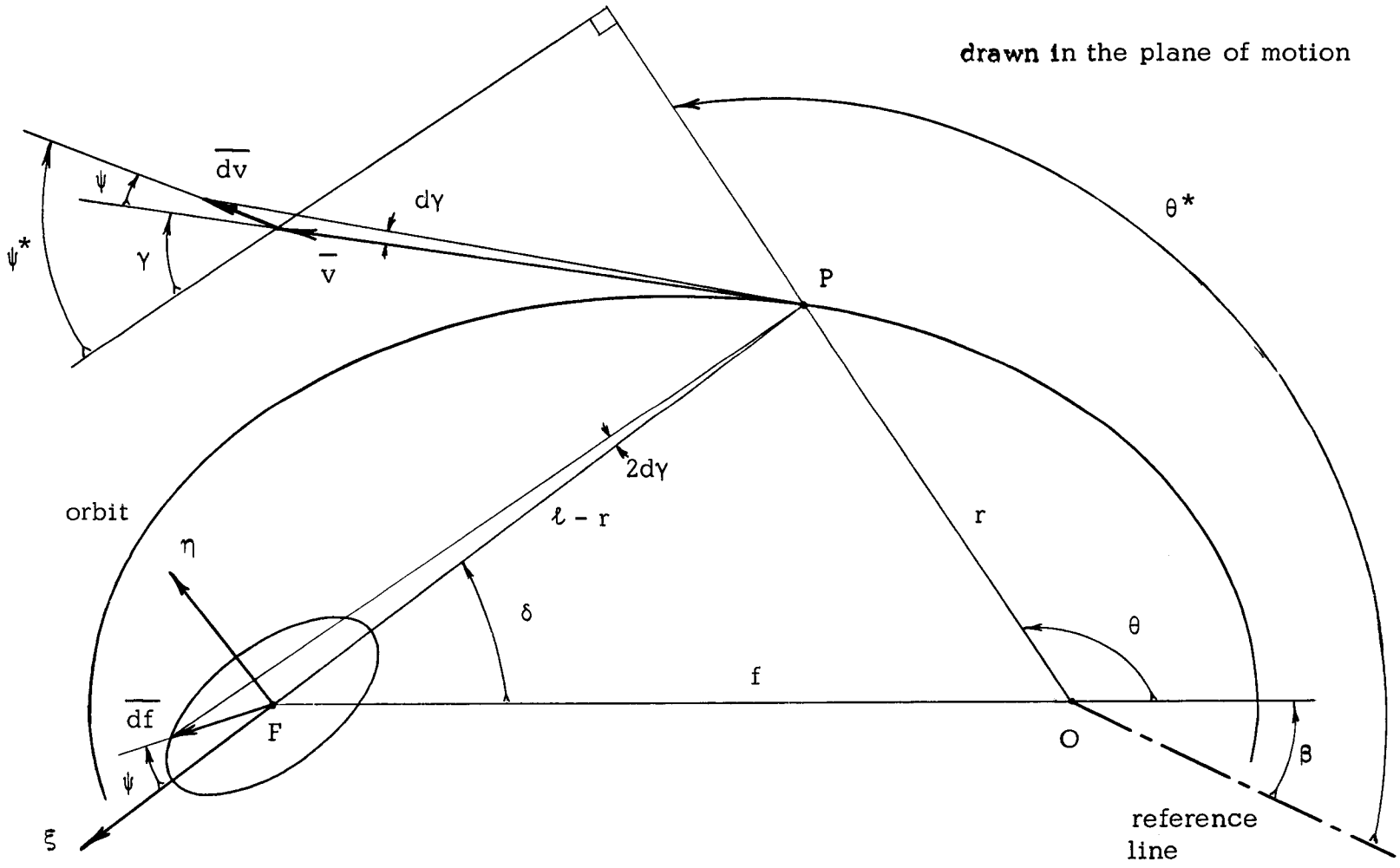

Figure 7. The notation of this analysis.

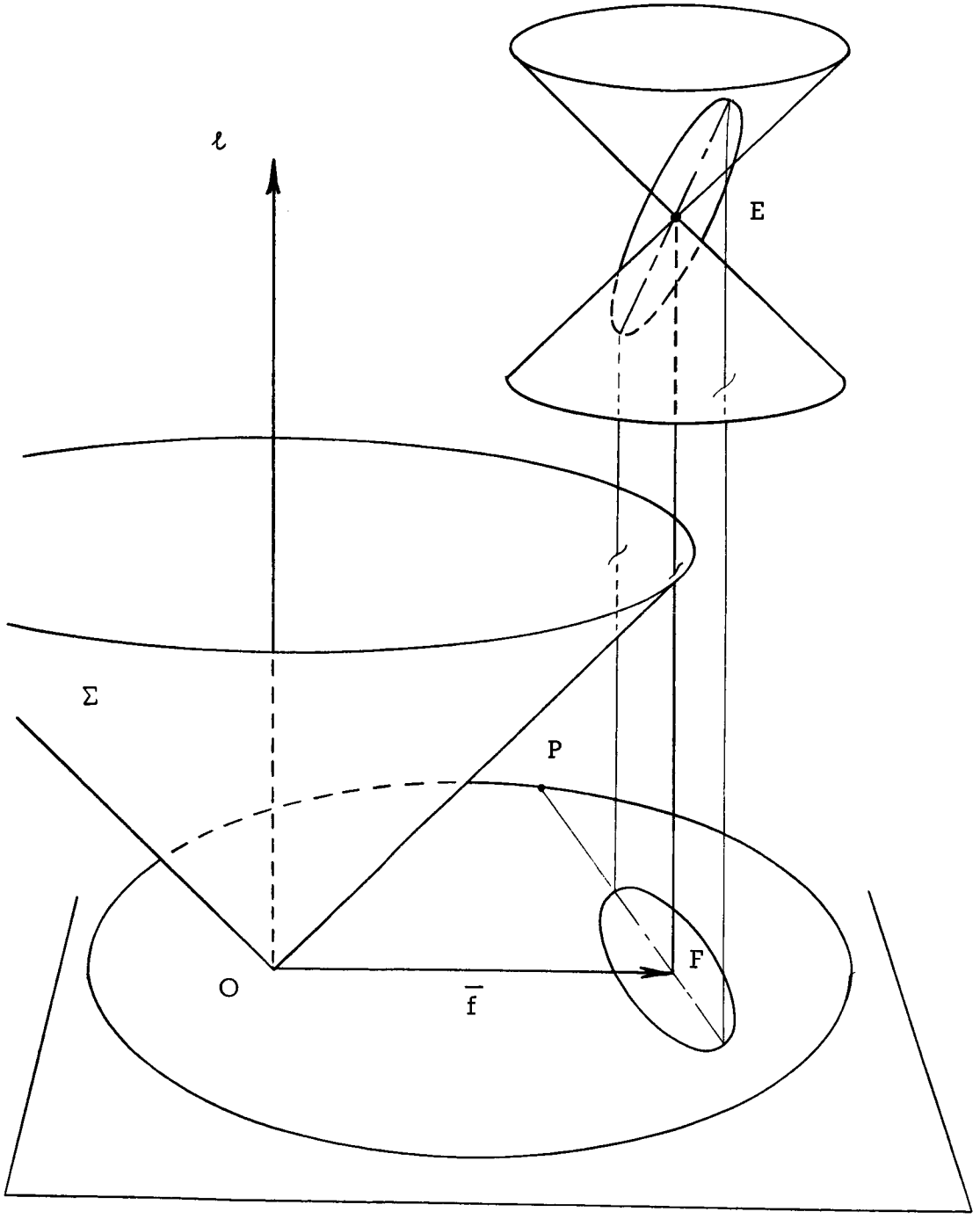

Figure 8. The variation of an orbit possible from one fixed position P.

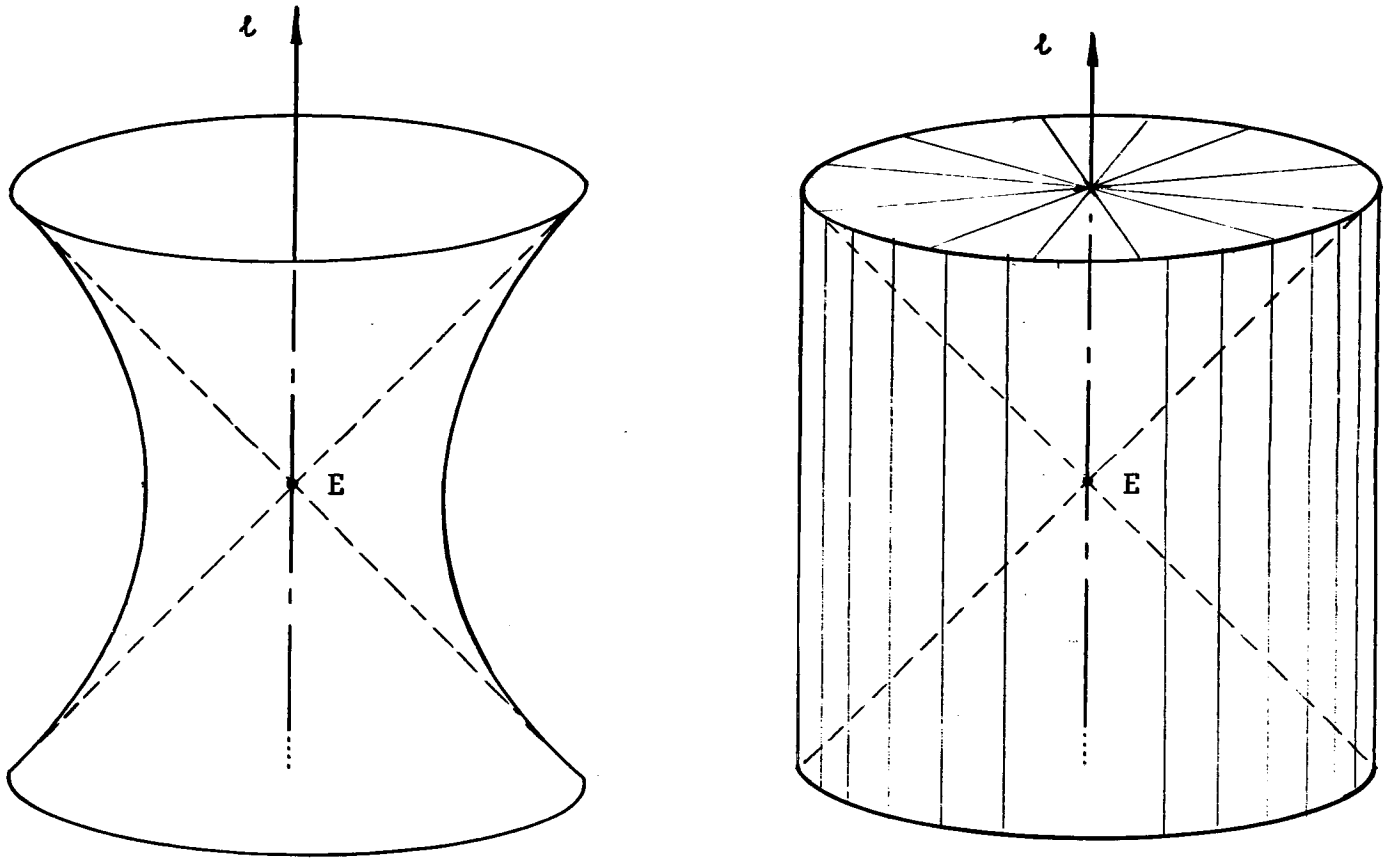

original

improved

Figure 9. The original and improved metric bodies for a circular orbit.

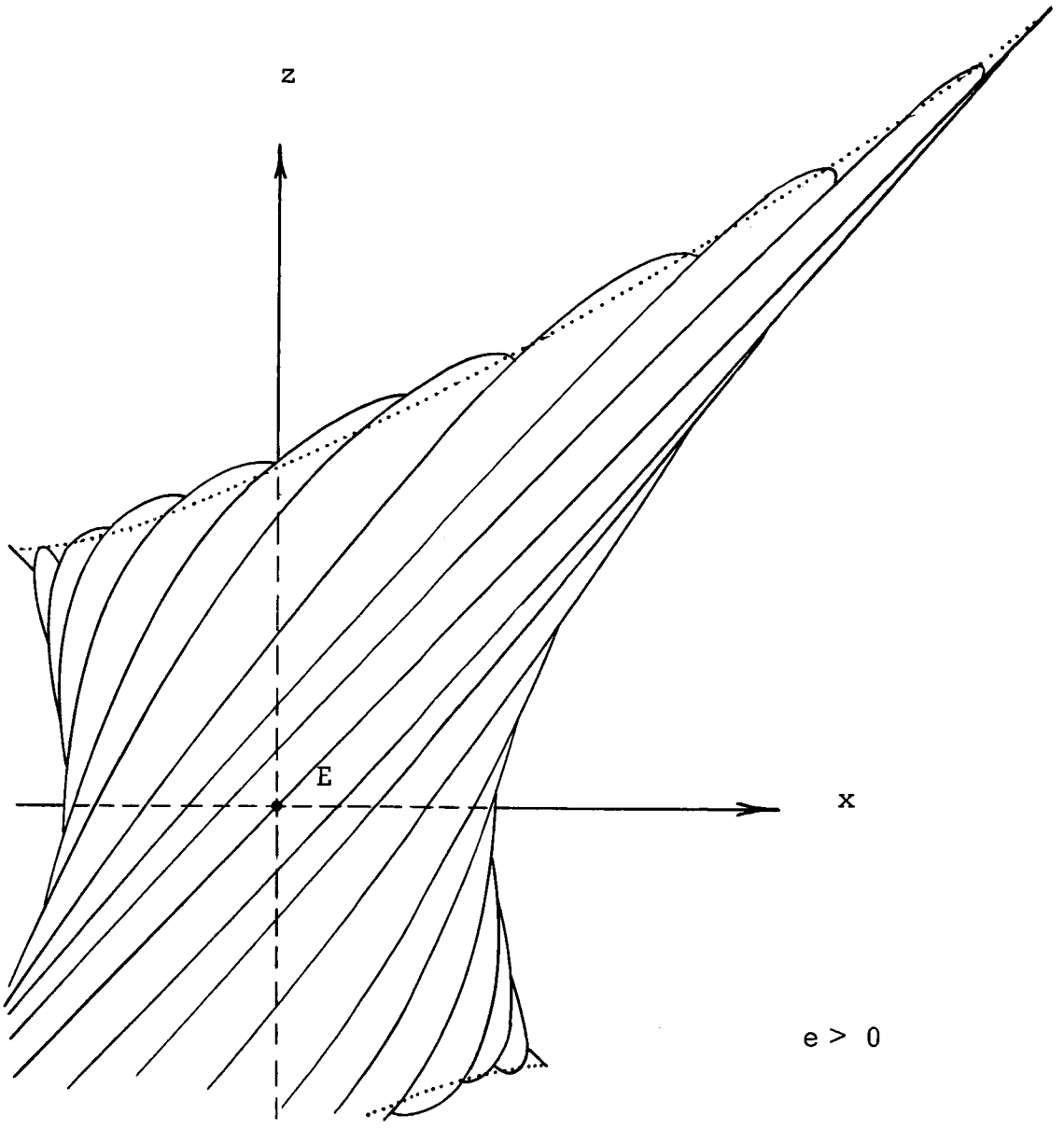

Figure 10. The side view of the original metric body.

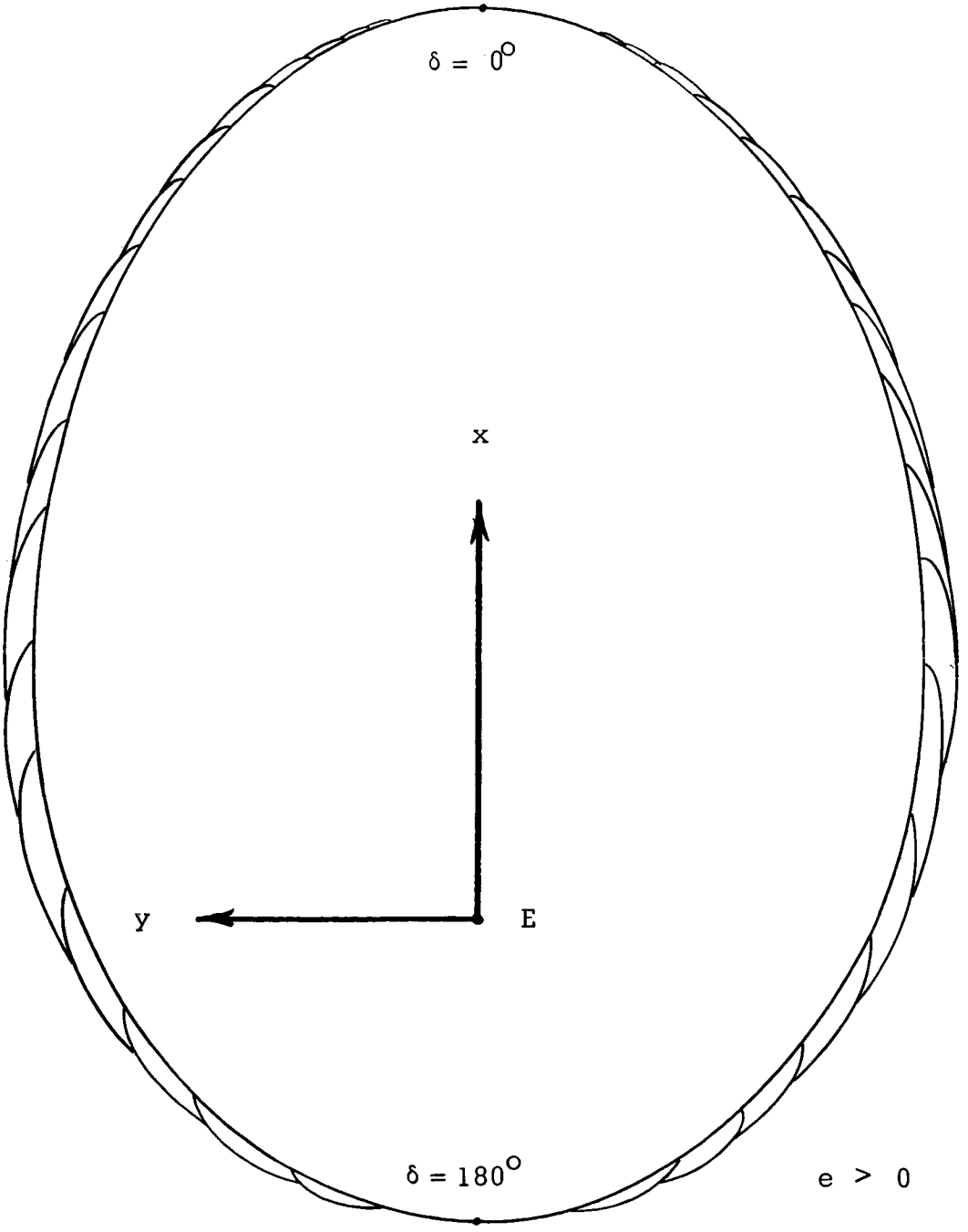

Figure 11. The top view of the original metric body, top half only.

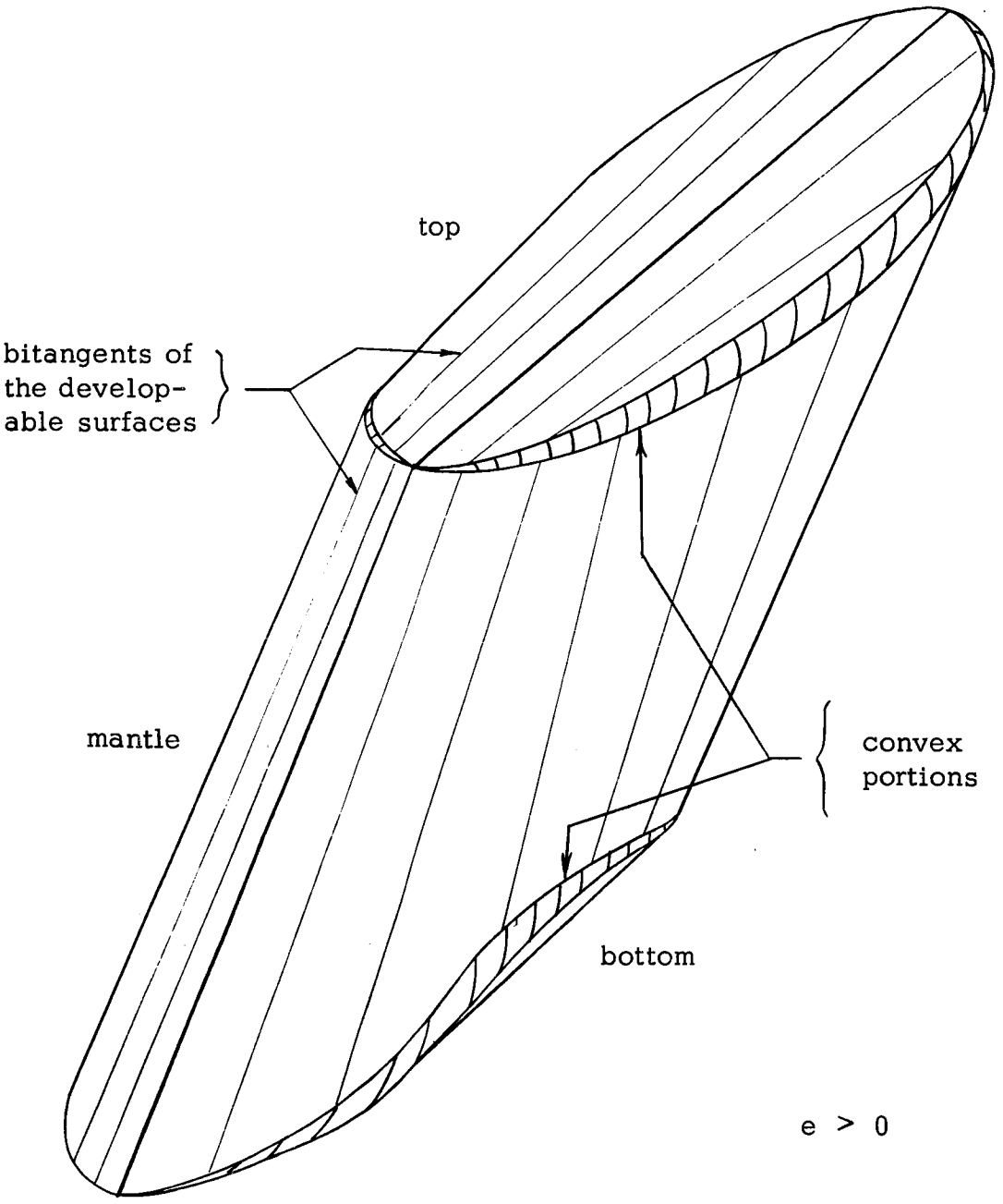

Figure 12. The improved metric body showing the convex portions and the developable surfaces.

c) The Tangent Planes

The first step in calculating the boundaries between the developable surfaces and the lips, the convex portions, is to determine the tangent planes of the original metric body. For this purpose it is convenient to establish a coordinate system in the metric body. This coordinate system is depicted in Figure 13. The origin is E, the point in configuration space representing the given ellipse. The x axis is taken parallel to the vector $\bar{f}$. The z axis is parallel to the ℓ axis of configuration space. The y axis is chosen so as to complete a right-hand orthogonal xyz coordinate system.

It should be observed that the z coordinate of a point on the metric body is equal to $d\ell$, the change in the length of the major axis. In the preceding section it was established that $d\ell$ is equal to the coordinate ξ. From the projection of the xy coordinates onto the $\xi\eta$ coordinates in Figure 14, the relation between the two sets of coordinates is readily evident. From these observations are found the parametric equations of the surface of the metric body.

$$x = \xi \cos\delta + \eta \sin\delta$$

$$y = \xi \sin\delta - \eta \cos\delta \qquad (20)$$

$$z = \xi$$

Thus, the surface of the metric body is given in terms of the intrinsic parameters ψ and δ by

$$\begin{aligned}\bar{\rho}(\psi,\delta) &\equiv x(\psi,\delta)\hat{i} + y(\psi,\delta)\hat{j} + z(\psi,\delta)\hat{k} \\ &= (\xi \cos\delta + \eta \sin\delta)\hat{i} \\ &+ (\xi \sin\delta - \eta \cos\delta)\hat{j} \\ &+ \xi\hat{k}\end{aligned} \tag{21}$$

where $\hat{i},\hat{j},\hat{k}$ are unit vectors in the x,y,z directions respectively and ξ and η are found in terms of ψ and δ from equations (19).

A vector normal to the surface of the metric body is given by the vector cross product

$$\bar{n} = \frac{\partial \bar{\rho}}{\partial \psi} \times \frac{\partial \bar{\rho}}{\partial \delta} \tag{22}$$

The only place $\bar{n}$ is the null vector is where the two vector derivatives on the right-hand side are aligned. This occurs only where both ψ is equal to zero, that is tangential impulse, and δ is such that the velocity vector of the orbit is horizontal. It will be seen that this causes no problem since in these cases the information sought is quite obvious.

Written out fully in terms of ψ and δ, the quantities of interest are as follows.

$$\frac{\bar{\rho}(\psi,\delta)}{R(1-e^2)^{1/2}} = \left[\frac{\cos\psi\cos\delta}{Z} + \frac{Z}{2(1-e\cos\delta)}\sin\psi\sin\delta\right]\hat{i}$$

$$+\left[\frac{\cos\psi\sin\delta}{Z} - \frac{Z}{2(1-e\cos\delta)}\sin\psi\cos\delta\right]\hat{j}$$

$$+\left[\frac{\cos\psi}{Z}\right]\hat{k} \qquad (23)$$

$$\frac{\partial\bar{\rho}}{\partial\psi}\frac{1}{R(1-e^2)^{1/2}} = \left[\frac{Z}{2(1-e\cos\delta)}\cos\psi\sin\delta - \frac{\sin\psi\cos\delta}{Z}\right]\hat{i}$$

$$+\left[-\frac{Z}{2(1-e\cos\delta)}\cos\psi\cos\delta - \frac{\sin\psi\sin\delta}{Z}\right]\hat{j}$$

$$+\left[-\frac{\sin\psi}{Z}\right]\hat{k} \qquad (24)$$

$$\frac{\partial\bar{\rho}}{\partial\delta}\frac{1}{R(1-e^2)^{1/2}} = \left\{\cos\psi\left[-\frac{\sin\delta}{Z}\left(1+\frac{e\cos\delta}{Z^2}\right)\right]\right.$$

$$+\sin\psi\left[\frac{1}{2(1-e\cos\delta)Z}\left[(Z^2\cos\delta)+e\sin^2\delta\cdot\right.\right.$$

$$\left.\left.\left.\cdot\left(1-\frac{Z^2}{(1-e\cos\delta)}\right)\right]\right]\right\}\hat{i}$$

$$+\left\{\cos\psi\left[\frac{1}{Z}\left(\cos\delta-\frac{e\sin^2\delta}{Z^2}\right)\right]\right. \qquad (25)$$

$$+\sin\psi\left[\frac{\sin\delta}{2(1-e\cos\delta)Z}\left[Z^2-e\cos\delta\cdot\right.\right.$$

$$\left.\left.\left.\cdot\left(1-\frac{Z^2}{1-e\cos\delta}\right)\right]\right]\right\}\hat{j}$$

$$+\left\{\cos\psi\left[-\frac{e\sin\delta}{Z^3}\right]\right\}\hat{k}$$

with $$R^2 \equiv \frac{2\ell^3 (dv)^2}{\mu}$$

$$Z^2 \equiv (1 + e^2 - 2e \cos \delta)$$

For a given ψ and δ, the vector $\bar{\rho}$ to the corresponding point Q on the surface of the metric body is found from equation (23), and a vector $\bar{n}$ normal to this surface at the point Q is produced by equation (22), where the derivatives called for are determined by equations (24) and (25). The tangent plane at Q is found as follows. If $\bar{\rho}'$ is a vector to any other point of the tangent plane at Q then the projections of $\bar{\rho}'$ and $\bar{\rho}$ on $\bar{n}$ are equal,

$$\bar{\rho} \cdot \bar{n} = \bar{\rho}' \cdot \bar{n} \qquad (26)$$

Therefore, the equation of the tangent plane is

$$x \frac{n_1}{\bar{\rho} \cdot \bar{n}} + y \frac{n_2}{\bar{\rho} \cdot \bar{n}} + z \frac{n_3}{\bar{\rho} \cdot \bar{n}} = 1 \qquad (27)$$

The plane is completely defined by the three constants which are the coefficients of x,y, and z in (27). These constants can be seen to be the reciprocals of the intercepts by the tangent plane of the x, y, and z axes, respectively. With the intercepts of the axes by the tangent plane labelled x_o, y_o, z_o, one may write

$$c_1 \equiv \frac{n_1}{\bar{\rho} \cdot \bar{n}} = \frac{1}{x_o}$$

$$c_2 \equiv \frac{n_2}{\bar{\rho} \cdot \bar{n}} = \frac{1}{y_o} \qquad (28)$$

$$c_3 \equiv \frac{n_3}{\bar{\rho} \cdot \bar{n}} = \frac{1}{z_o}$$

These three constants are used to specify the tangent planes of the metric body. These constants are well-suited for this purpose since, while the tangent planes are frequently parallel to one or more of the coordinate axes, they do not approach arbitrarily close to the origin. Thus, these three constants will range through values in a finite interval about zero. As will be seen, this interval has a length on the order of the size of R, defined after equation (25).

The points of the top half of the metric body, for which z is positive, can be put into congruence with the points of the bottom half of the body, for which z is negative, by a rotation of 180 degrees about the y axis. In addition, the metric body is symmetric with respect to the xz plane. The entire body can then be generated by the quarter of the body in the region where y and z are positive. From this quarter the quarter in the region where y is negative and z is positive is generated by the mapping

$$(x, y, z) \rightarrow (x, -y, z) \qquad (29)$$

This completes the top half of the body. From this top half, the bottom half is constructed by mapping

$$(x, y, z) \rightarrow (-x, y, -z) \ , \tag{30}$$

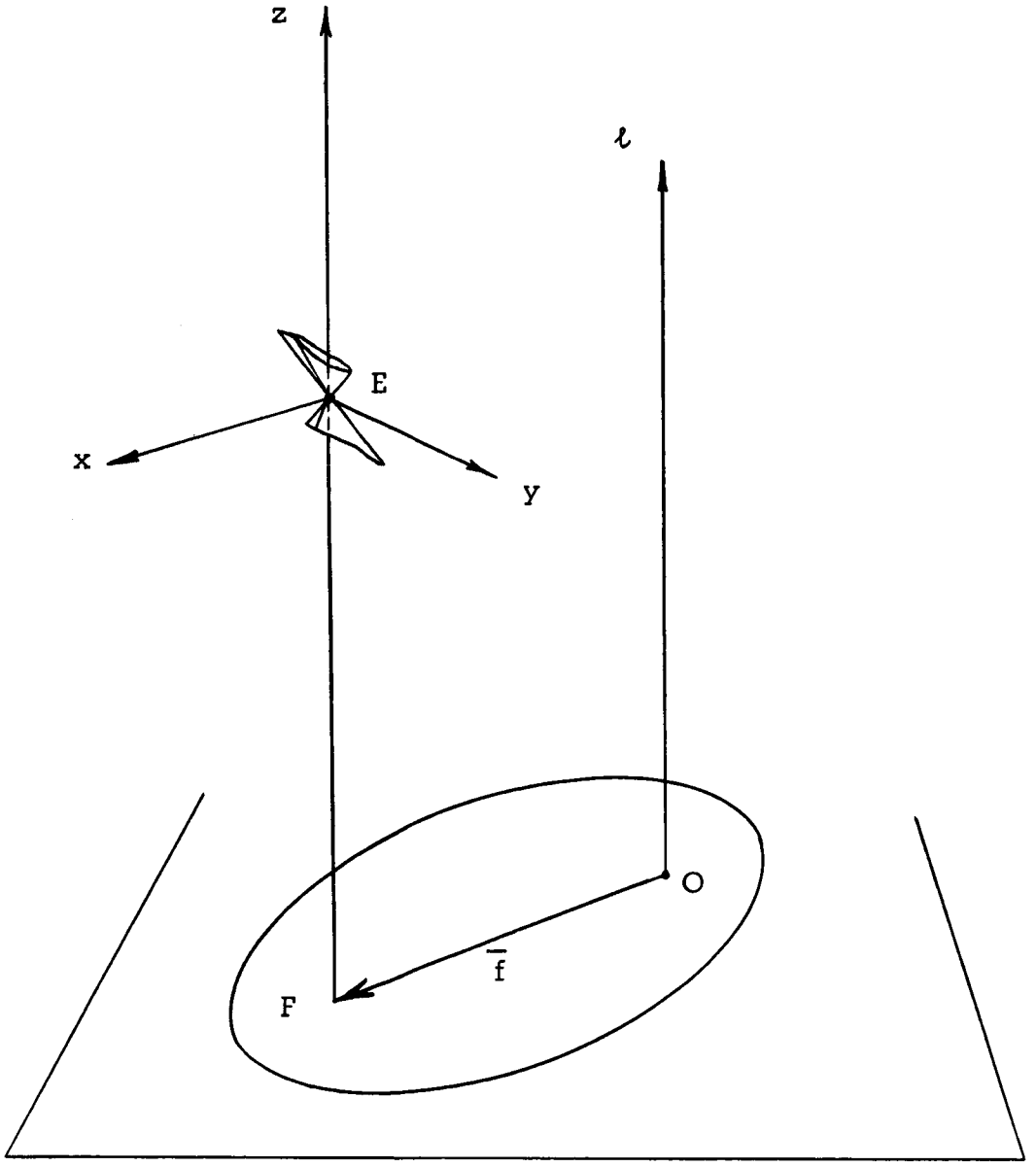

Figure 13. The coordinate system in the metric body.

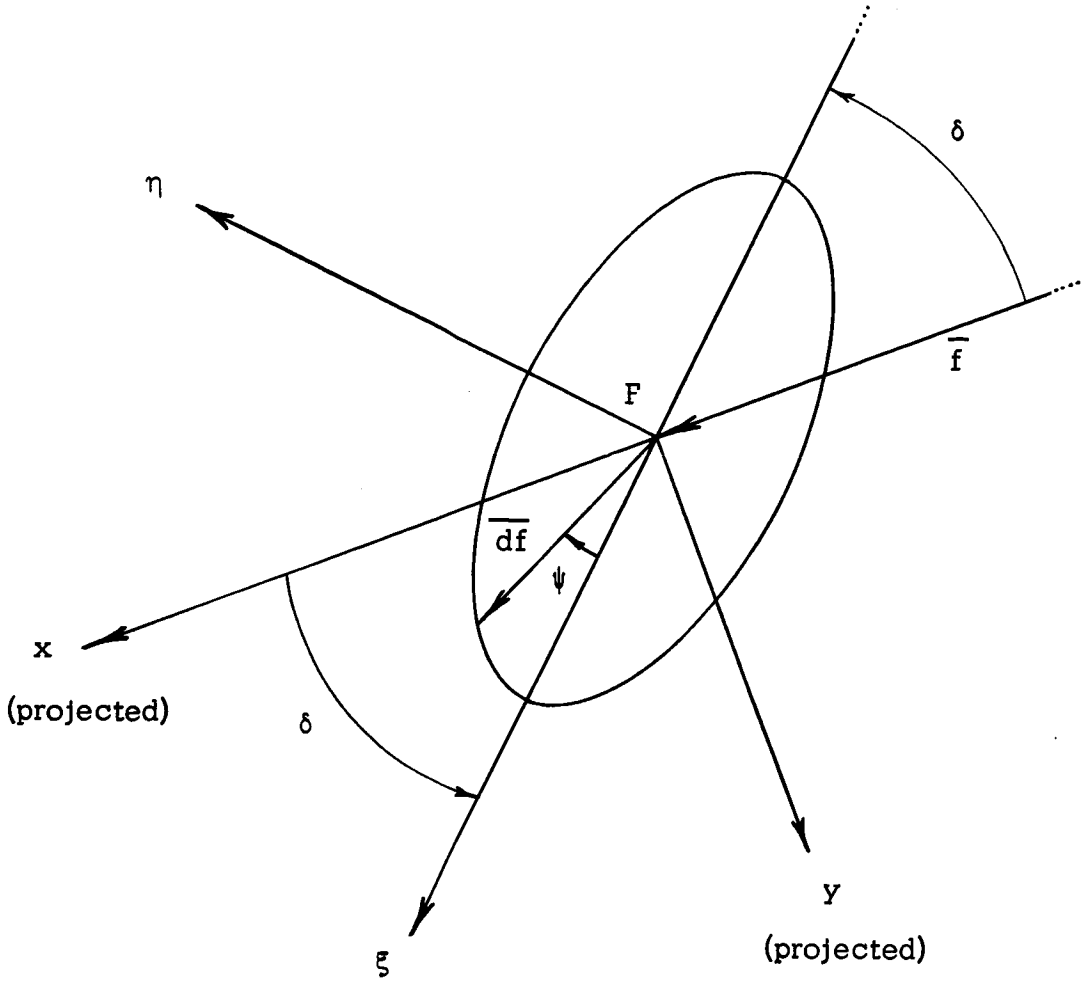

Figure 14. The relation between $\xi\eta$ and xy coordinate systems.

d) The Bitangents

The bitangents which form the developable surfaces which bridge the concave portions of the metric body are made by planes which are tangent to the metric body at two different points. The bitangent is the line in this plane joining the points of tangency.

In some cases this approach to the developable surface must be replaced by a more basic approach as discussed previously. These cases occur at points corresponding to both an horizontal velocity vector and a tangential impulse. At such points the metric body does not have a well-defined tangent plane. These points correspond only to tangential impulses and at the apses of elliptical orbits or around the entire orbit if it is circular. The elements of the developable surface in the latter case are depicted in Figure 9. For the elliptical orbits these points of tangential thrust at the apses combine with one another (Figure 15) to form the subgroup of the Hohmann type of maneuvers. It is evident that these cases present no problem, but are actually simpler to handle than the general points. For these cases use of the definition of convexity of the body (the body is convex if it contains all the points on the straight line between any two of its points) leads to the simple constructions shown.

These simple connections lie in the developable surfaces of the metric body. To find the bitangents which make up the rest

of the developable surfaces, one must find sets of two different points given by $\bar{\rho}_1$ and $\bar{\rho}_2$ which have the same tangent plane. As $\bar{\rho}$ varies generating the surface of the metric body, the constants used to define the tangent plane sweep out a surface in the three space c_1, c_2, c_3. The parameters of this surface are ψ and δ. The bitangents are represented by points of this surface to which correspond two distinct sets of ψ and δ. Thus, what is sought is where this surface in c_1, c_2, c_3 space intersects itself.

The points of self-intersection are found by slicing the space with a plane and examining the trace of the surface on the plane for intersections. The cross sections selected are planes of constant c_2. This choice is made in view of the particularly predictable behavior of the y intercept of the tangent planes. For the quarter of the body with y and z both positive the tangent planes which produce the developable surface forming the mantle have c_2 which begins at zero for δ equal to zero, increases to a finite maximum, and then decreases again to zero at δ equal to 180 degrees. In this same quarter the tangent planes which produce the top developable surface have c_2 which begin at zero, corresponding to the simple connection between δ equal to zero and 180 degrees lying in the xz plane, and gradually increasing to a finite maximum. Thus, pertinent planes of constant c_2 can be selected quite easily.

As was noted in the preceding section, properties of the entire body can be obtained from knowledge of the body in the single quarter where y and z are positive by using (29) and (30). It is only necessary, therefore, to compute the half of the top and the half of the mantle where y is positive. In the part of any of the developable surfaces which has y positive a bitangent connecting (ψ_1, δ_1) with (ψ_2, δ_2) has an image bitangent with y negative connecting (ψ'_1, δ'_1) with (ψ'_2, δ'_2). The image points are given by the relations corresponding to (29):

$$\psi' = -\psi$$
$$\delta' = -\delta \qquad (31)$$

This gives the other half of the top developable surface.

Similarly, a point in the top half of the body given by (ψ, δ) has a corresponding point in the bottom half given by (ψ', δ') found through the relations corresponding to (30):

$$\psi' = 180^{\circ} - \psi$$
$$\delta' = -\delta \qquad (32)$$

Thus, a bitangent in the top developable surface yields a corresponding bitangent in the bottom surface.

A combination of (31) and (32) is used to find the bitangents

which form the mantle. Equation (32) is employed to find the bitangents of the half of the mantle with y positive, and equation (31) generates the other half.

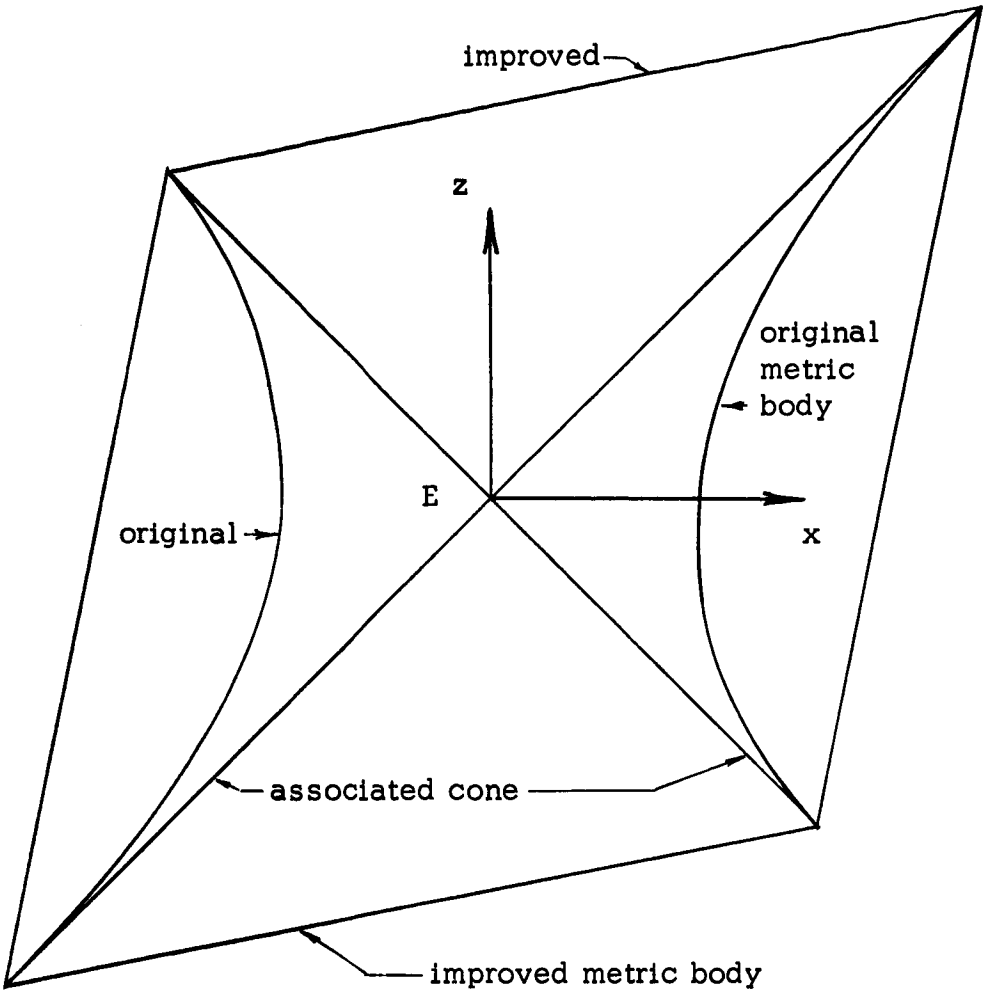

e = .2

Figure 15. The trace in the xz plane of the metric bodies.

e) Method of Computation

As discussed in the previous section, there is a surface in the three space c_1, c_2, c_3 which represents the tangent planes of the metric body. Determining the bitangents is equivalent to finding the points where this surface intersects itself. These self-intersections are found by slicing the space by planes of constant c_2, which means constant y_o.

This is accomplished numerically on the high speed digital computer (an IBM 7044) of the Graduate School Computing Center of the University of Colorado. The details of the computation are as follows.

1. Only the edge in the quarter where y and z are positive is calculated. Thus, the range of δ is 0 to 180 degrees, and the range of ψ is 0 to 90 degrees.
2. A fixed value of c_2 is given. This determines the plane used to slice the space.
3. Next, δ is held fixed while ψ varies until the given value of c_2 is acquired to within $\pm$ .0000001 in units of $R(1 - e^2)^{1/2}$. This represents a point of the trace of this surface in the given c_2 plane.
4. The trace is completed by repeating step 3 for different values of δ from 0 to 180 degrees. The increments

in δ vary from 0.25 to 2 degrees, with the differing step size suggested by the need for uniform accuracy.

5. Straight line interpolation between points of the trace is used to find the self-intersections which yield the bitangents of the top developable surface.

6. When an intersection is found by step 5, additional points are calculated by step 3 to give the desired accuracy. Extremely high accuracy is obtained with only one iteration. Frequently this accuracy extends nearly to the eight place accuracy of the single precision trigonometric functions of the computer.

7. To find the bitangents which form the mantle, the trace obtained in step 4 is overlaid by the trace obtained from it by substituting $-x$ and $-z$ for x and z. That is, transformations (30) and (32) are used. The intersections are then found as in steps 5 and 6.

f) Variation of Elements

From Figure 7 it can be observed that, for an impulse the direction and position of which are defined by ψ and δ, the change in $\bar{f}$ normal to $\bar{f}$ is given by

$$\overline{df} \perp \bar{f} = \eta \cos\delta - \xi \sin\delta \tag{33}$$

Also, it is apparent that the change in θ is the negative of the change in β.

$$d\theta = -d\beta \tag{34}$$

The change in β is

$$d\beta = \frac{\xi \sin\delta - \eta \cos\delta}{f} \tag{35}$$

Therefore, the change in θ is

$$d\theta = \frac{\eta \cos\delta - \xi \sin\delta}{f} \tag{36}$$

Similarly, the change in $\bar{f}$ in the direction $\bar{f}$ is given by

$$\hat{f} \cdot \overline{df} = df \tag{37}$$

$$df = \eta \sin\delta + \xi \cos\delta \tag{38}$$

Now, using equations (19) for ξ and η in equations (8) and (13) for $d\ell$, equations (36) and (38) for $d\theta$ and df, and defining a

new independent variable u by

$$u \equiv v\left[\frac{L}{\mu}\right]^{1/2} \tag{39}$$

where L is some reference unit of length, one obtains the equations for the variation of the elements in the form:

$$\frac{d\ell}{du} = \ell\left[\frac{2\ell\,(1-e^2)}{1+e^2-2e\cos\delta}\right]^{1/2} \cos\psi \tag{40}$$

$$\frac{d\theta}{du} = \frac{1}{e}\left[\frac{2\ell\,(1-e^2)}{1+e^2-2e\cos\delta}\right]^{1/2}\left[\frac{1+e^2-2e\cos\delta}{2(1-e\cos\delta)}\sin\psi\cos\delta - \right.$$

$$\left. - \cos\psi\sin\delta\right] \tag{41}$$

$$\frac{df}{du} = \ell\left[\frac{2\ell\,(1-e^2)}{1+e^2-2e\cos\delta}\right]^{1/2}\left[\frac{1+e^2-2e\cos\delta}{2(1-e\cos\delta)}\sin\psi\sin\delta + \right.$$

$$\left. + \cos\psi\cos\delta\right] \tag{42}$$

Equation (42) can conveniently be replaced, since e is f/ℓ, by

$$\frac{de}{du} = \left[\frac{2\ell\,(1-e^2)}{1+e^2-2e\cos\delta}\right]^{1/2}\left[\frac{1+e^2-2e\cos\delta}{2(1-e\cos\delta)}\sin\psi\sin\delta + \right.$$

$$\left. + \cos\psi\,(\cos\delta - e)\right] \tag{43}$$

The angles θ and δ can be related (Figure 7) by using equation (16) and a similar expression also obtained from the law of cosines.

$$\frac{v^2 \ell}{2\mu} = \frac{1 + e^2 + 2e \cos \theta}{1 - e^2} \tag{44}$$

Equating (16) and (44) gives a relation between $\cos \theta$ and $\cos \delta$.

$$\cos \theta = \frac{1}{2e} \left[\frac{(1 - e^2)^2}{1 + e^2 - 2e \cos \delta} - (1 + e^2) \right] \tag{45}$$

The law of sines relates $\sin \theta$ and $\sin \delta$.

$$\sin \theta = \sin \delta \frac{\ell - r}{r} \tag{46}$$

Using the energy integral (4) and equation (16) one obtains

$$\sin \theta = \sin \delta \frac{(1 - e^2)}{1 + e^2 - 2e \cos \delta} \tag{47}$$

Equations (45) and (47) can be inverted to give expressions for $\sin \delta$ and $\cos \delta$.

$$\sin \delta = \sin \theta \frac{(1 - e^2)}{1 + e^2 + 2e \cos \theta} \tag{48}$$

$$\cos \delta = \frac{1}{2e} \left[1 + e^2 - \frac{(1 - e^2)^2}{1 + e^2 + 2e \cos \theta} \right] \tag{49}$$

The flight path angle γ is given by either of the following.

$$\tan \gamma = \frac{e \sin \theta}{1 + e \cos \theta} \tag{50}$$

$$\tan \gamma = \frac{e \sin \delta}{1 - e \cos \delta}$$

During an impulsive velocity change the angles θ^* and ψ^* remain constant (Figure 7). These are given by

$$\theta^* = \theta + \beta \tag{51}$$

$$\psi^* = \psi + \gamma \tag{52}$$

For this reason it is practical to use ψ^* in place of ψ as the more natural control parameter. Equation (51) for θ^* has already been used in obtaining (34).

The equations for the variation of the elements of the orbit, (40), (41), (42), and (43), along with equations (48), (49), (50), and (52) provide a complete description of the effects of an impulsive change of velocity. These equations are used to determine the magnitude an impulse can have while continuing to satisfy the necessary condition for optimal impulse.

g) Multiple Impulse Trajectories

Multiple impulse trajectories made up of impulses which everywhere satisfy the necessary condition and which are joined in an optimal fashion can be generated by using the equations for the variation of elements in the preceding section. This generation is accomplished in the following manner.

1. The initial orbit is fixed in configuration space by e, ℓ, and β, or what is the same, by ℓ and $\bar{f}$.
2. The initial impulse is fixed in position and direction by θ^* and ψ^*. This position and direction must be such that initially this impulse satisfies the necessary condition for optimality. That is, the point representing it in configuration space must lie on a convex portion of the metric body.
3. The equations for the variation of elements are integrated numerically and the point representing the impulse is followed across the metric body until it reaches the boundary of the convex portion. This boundary is formed by the end points of the bitangents composing the developable surfaces which cover the concave portions of the metric body.

4. When the boundary of the convex portion is crossed, the impulse is terminated and the magnitude of that impulse is fixed.

5. The next impulse used is the one represented by the point at the other end of the bitangent. With this impulse, steps 3, 4, and 5 are repeated.

It may be noted that whenever a tangential impulse satisfies the necessary condition, it continues to do so until escape velocity is reached. As pointed out previously, a tangential thrust is a possible optimum only when the velocity vector is horizontal.

It should be clear from the construction of the improved metric body that a connection between two impulses can be optimal only if the connection is between impulses represented by the opposite endpoints of a bitangent in a developable surface on the improved metric body. First of all both impulses must be represented throughout by points in the convex portion of the metric body. If at the junction either one of the impulses lies in the interior of the convex portion of the metric body, then by the insertion of a third impulse across the connection with the other impulse it will be possible to reduce the characteristic velocity of the maneuver. This is evident from the fact that the arcs representing the two impulses in configuration space meet at an angle other than 180 degrees. With full freedom to move one of

the impulses in any direction, this corner can easily be cut. At the junction, if both impulses are on the boundary, but not on the same bitangent, then the corner can be cut, though more than one additional impulse may be required. This is all inherent in the construction of the improved metric body, which is completely convex.

The net result of the above is that two impulses can be joined in an optimal fashion only if at the junction they are represented by points on the metric body at opposite endpoints of a bitangent member of one of the developable surfaces, or if one represents simply a continuation of the other. This is, in effect, a corner condition for this problem. It is a requirement of the type which permits corners as long as they are of a particular class. If the original body were entirely convex, then no corners at all would be permissible. The presence of the concave portions which must be made convex makes permissible this one class of corner.

Thus, a multiple impulse arc in this configuration space may possibly be optimal only if all the corners between impulsive arcs are of this bitangent type, and if all of the arcs themselves satisfy the previously discussed necessary condition for optimal impulses.

There is one maneuver in the large which, because of its simplicity, should be used as a check against any maneuver

regardless of the number of impulses used. This is the four impulse transfer between elliptical orbits consisting of an escape from periapsis of one orbit, entry at periapsis of the final orbit, and two negligible impulses at infinity to provide the proper orientation[10,11]. If this maneuver between any two points of the multiple or single impulse arc in configuration space has a characteristic velocity less than that associated with following the arc, then obviously the arc under consideration has been defeated in the large. The four impulse transfer can then replace all or part of this arc at a savings in characteristic velocity.

The characteristic velocity of the four impulse transfer between two orbits can readily be calculated from the expression for the impulse required to transfer at the periapsis of an ellipse to a tangential parabolic escape trajectory.

$$\min \Delta u_{esc.} = (u \text{ escape} - u)_{\text{periapsis}}$$

$$\min \Delta u_{esc.} = \frac{1}{[\ell(1 - e)]^{1/2}} \left[2 - (2[1 + e])^{1/2} \right] \tag{53}$$

The characteristic velocity of the four impulse transfer between two orbits is the sum of this quantity for each of the two orbits.

III. RESULTS

a) Results of Computations

The computations, carried out as previously described, yield their results in two forms. The set of impulses specified by a given position and direction but of infinitesimal magnitude which satisfy the necessary condition for optimality is determined, and also the pairs of endpoints of bitangents corresponding to permissible corners are found.

For the final results it is natural to use θ, the angular position on the ellipse measured from periapsis with the attracting body as vertex, and ψ^*, the angle measured up from the local horizontal, to describe the position and direction of an impulse (Figure 7). The shape of the metric body is dependent only on the eccentricity e. Therefore, all infinitesimal impulses which satisfy the necessary condition for optimality are represented by points in the three space ψ^*, θ, e. It is found that these points, which correspond to all points lying on convex portions of all metric bodies in the configuration space, form a compact region in the space ψ^*, θ, e. This region is illustrated in Figure 16. The region has polar symmetry in planes parallel to the $\psi^*\theta$ plane, so the entire region can be represented by drawing only the part for $0 \leq \theta \leq 180^{\circ}$.

The bounding surface of this region represents the points on the metric body separating the convex and concave portions. These points are the endpoints of the bitangents used to render the original

metric body convex. In Figure 16 the upper boundary, the farther from the θe plane, represents the endpoints of the bitangents forming the top or the bottom developable surfaces. The boundary nearer the θe plane corresponds to the endpoints of the bitangents forming the mantle of the metric body. This may be better visualized by referring to the improved metric body in Figure 12.

A useful means of presenting this region is to display cross sections of the region produced by planes of constant eccentricity, e. This is done in Figures 17a through 17i. The cross sections are calculated for e varying from 0 to .9 in steps of one-tenth. From these figures the directions of impulse ψ^* which satisfy the necessary condition for optimality for a given position θ on an ellipse of eccentricity e can easily be read. In these figures ψ^* must be such that the point (ψ^*,θ,e) lies on or between the two lines drawn. These lines are the traces of the boundaries of the region described in Figure 16.

Once an impulse of direction ψ^* and position θ originating from an initial orbit of eccentricity e is selected so that with a sufficiently small magnitude it satisfies the necessary condition for optimality, the obvious next step is to determine to what magnitude this impulse can be continued and still satisfy this necessary condition. Throughout an impulse ψ^* remains constant. Therefore, as the infinitesimal metric body moves along the arc in configuration

space produced by the continuation of this impulse, the point in (ψ^*, θ, e) space representing the forward point where the arc pierces the metric body moves in a plane of constant ψ^*. For the purpose of determining at what magnitude an impulse ceases to satisfy the necessary condition of optimality it is, therefore, convenient to present the region in Figure 16 by slicing it along planes of constant ψ^*.

Figures 18a through 18j depict cross sections of constant ψ^* of this region for ψ^* from 0 to 20 degrees in steps of 2 degrees. The cross section for ψ^* equal to zero is simply the e axis, the θ axis, and a line parallel to the e axis at θ equal to 180 degrees, as can be readily seen from Figure 16. As noted previously, this is just the group of the Hohmann type of transfers. An impulse in this group can be continued until escape velocity is attained without ever ceasing to satisfy the necessary condition for optimality.

In these figures only those points (ψ^*, θ, e) lying on or between the two lines represent impulses which, for a sufficiently small magnitude, satisfy the necessary condition. As these figures are drawn, the lower line represents points on the boundary of the top or bottom developable surfaces of the metric body, while the upper line represents points on the boundary of the mantle, or side developable surface of the metric body.

The pairs of endpoints of bitangents corresponding to

permissible corners in multiple impulse arcs are given in Figures 19 and 20. These pairings are given by curves of constant e drawn on a graph which has two θ axes, one representing the θ value at one end of the bitangent, the other representing the θ value at the other end of the bitangent. These curves are just level curves of a surface in the space of (e, θ_1, θ_2). Figure 19 represents the top and bottom developable surfaces. Figure 20 represents the side developable surface. It should be noted that the roles of θ_1 and θ_2 are completely interchangeable.

With every point from the curves in these figures are associated the two values of θ, one from each axis. Associated with each of these values of θ is a value of ψ^* obtained from the curves in Figures 17a through 17i.

From Figure 19 for the top or bottom developable surfaces a set (e, θ_1, θ_2) is taken to the proper Figure 17 determined by e, and for θ_1 and θ_2, ψ_1^* and ψ_2^* are read from the upper line. The left-hand scale is used for the top developable surface of the metric body, the right-hand scale is used for the bottom developable surface.

Similarly, from Figure 20 for the mantle of the metric body a set (e, θ_1, θ_2) is taken to the Figure 17 determined by e, and corresponding to θ_1 and θ_2, ψ_1^* and ψ_2^* are read from the lower line. The top edge of the mantle is read on the left-hand scale, the bottom edge is read from the right-hand scale.

In summary, one has two simply connected surfaces in the space (e,θ_1,θ_2), and two corresponding simply connected surfaces in the space (ψ^*,θ,e) which form the boundary of a compact region representing all infinitesimal impulses which satisfy the necessary condition for optimality. Every point on one of the surfaces in the space (e,θ_1,θ_2) has two associated points on the corresponding surface in the space (ψ^*,θ,e). This association provides the pairs (ψ_1^*, θ_1), (ψ_2^*,θ_2) which are endpoints of the bitangents of the developable surfaces of the metric body.

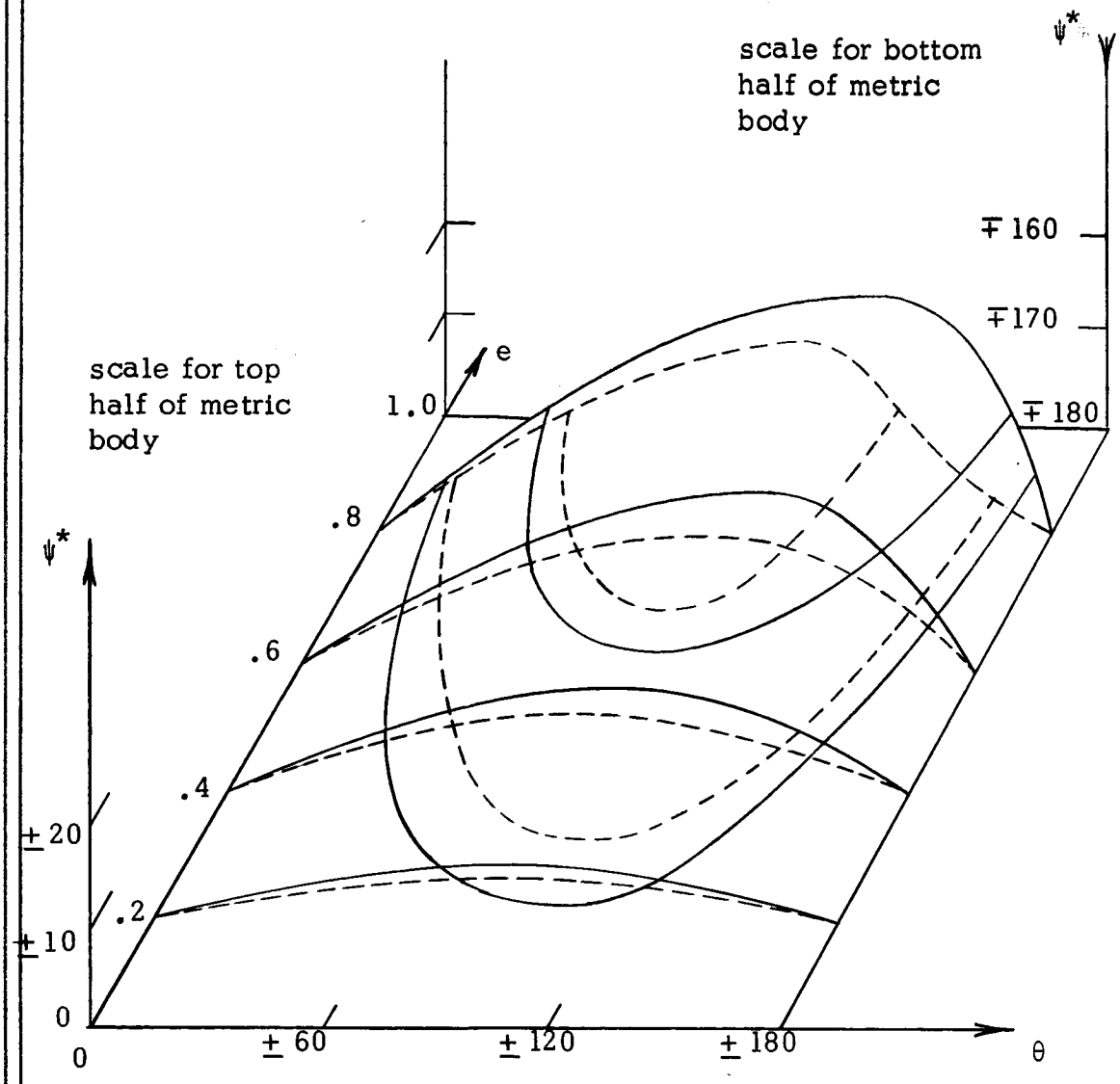

1 Upper surface (solid lines) represents the boundary of the top and bottom developable surfaces.

2 Lower surface (dashed lines) represents the boundary of the side developable surface, the mantle.

Figure 16. The region satisfying the necessary condition.

all angles in degrees

Left-hand scale is for top half of the metric body (increasing energy).

Right-hand scale is for bottom half of the metric body (decreasing energy).

e = .1

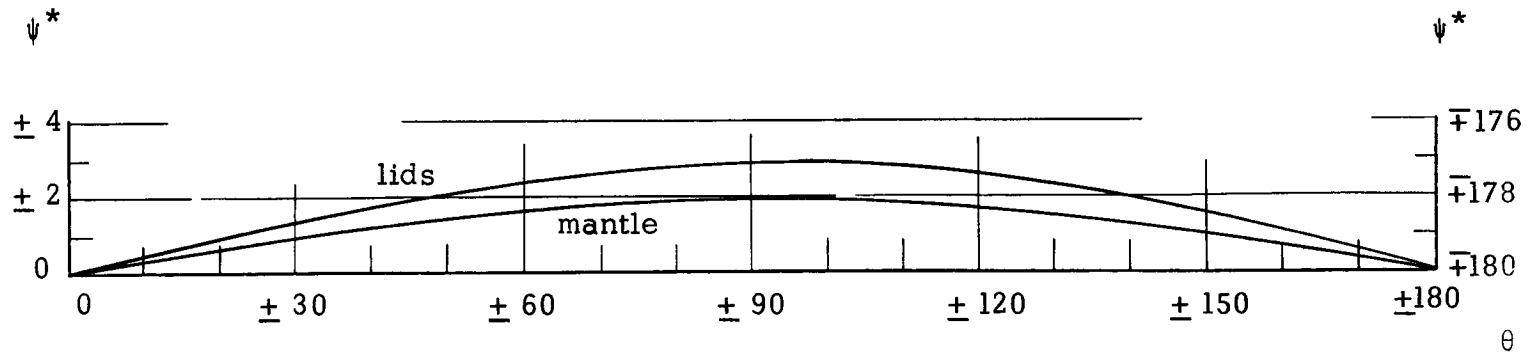

Figure 17a.

Figure 17. Directions of impulse which satisfy the necessary condition, for fixed e and various θ.

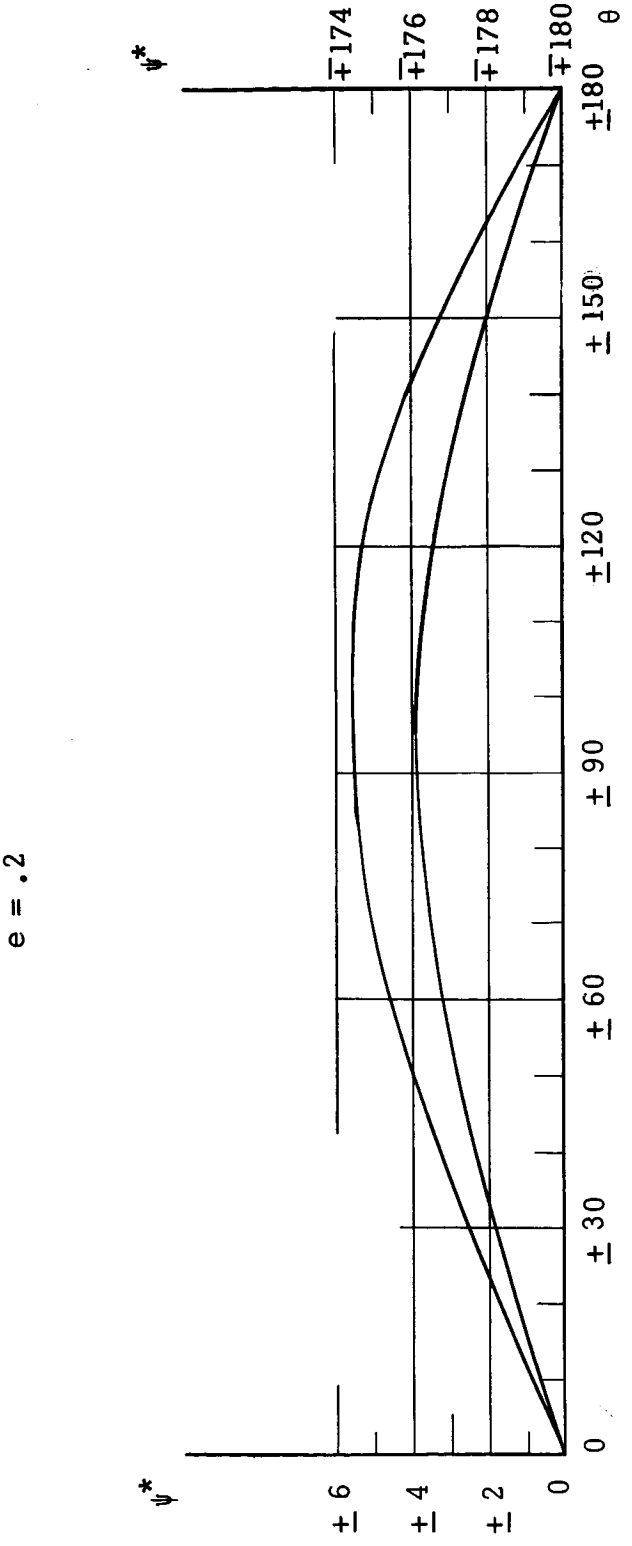

Figure 17b.

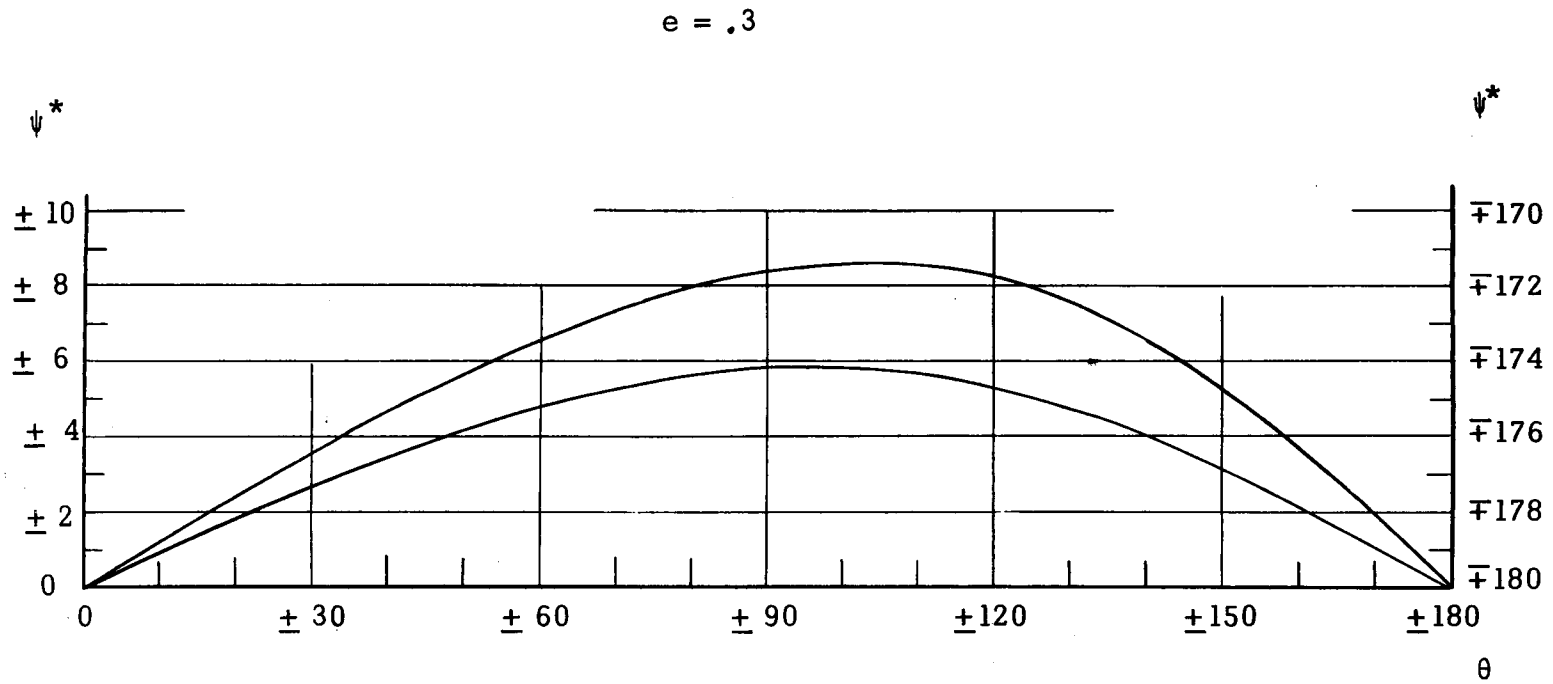

Figure 17c

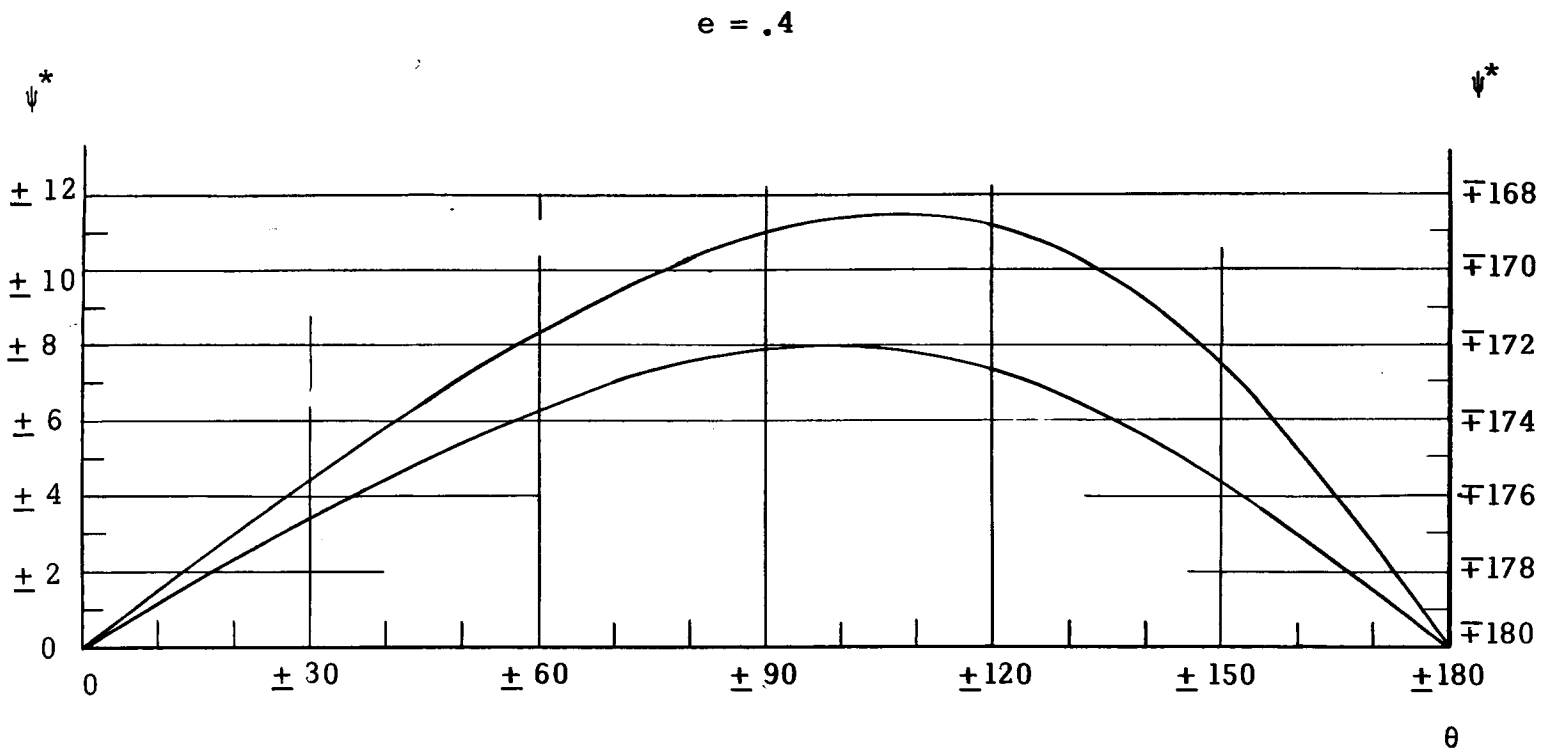
e = .4
ψ*
ψ*
± 12
± 10
± 8
± 6
± 4
± 2
0
∓168
∓170
∓172
∓174
∓176
∓178
∓180
0
± 30
± 60
± 90
±120
± 150
±180
θ

Figure 17d.

e = .5

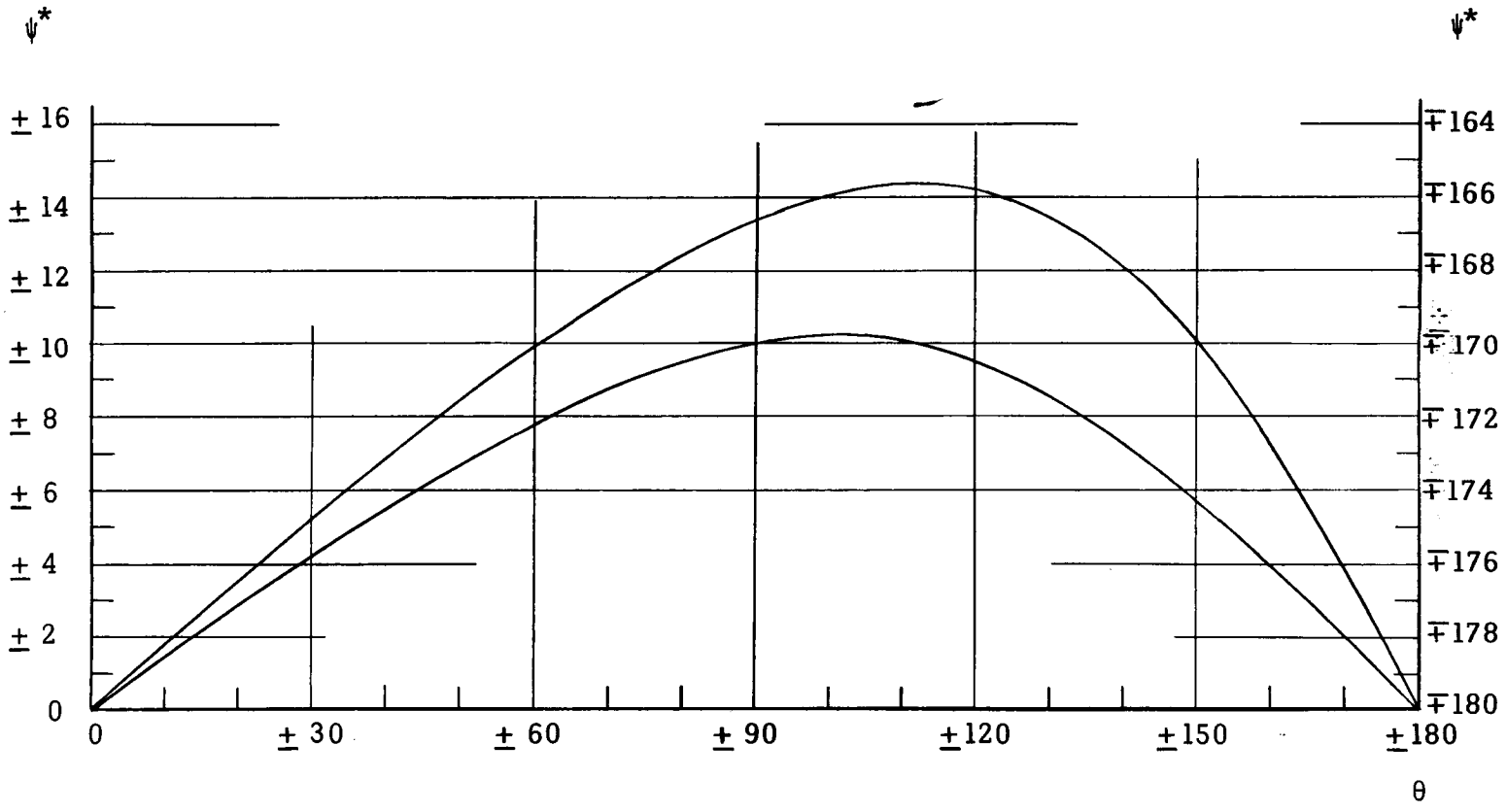

Figure 17e.

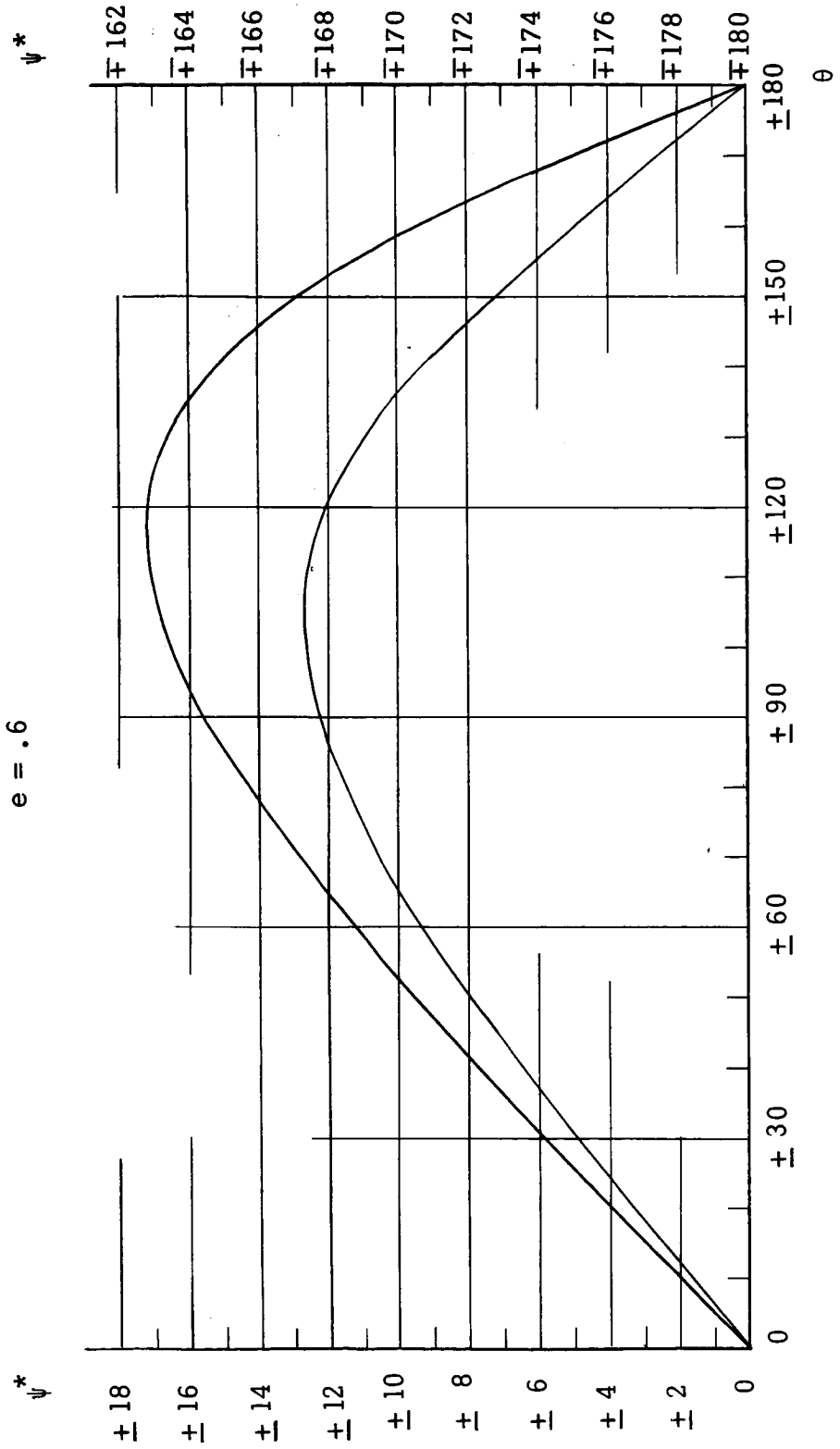
e = .6
ψ*
ψ*
θ
0
± 2
± 4
± 6
± 8
± 10
± 12
± 14
± 16
± 18
0
± 30
± 60
± 90
± 120
± 150
± 180
∓ 162
∓ 164
∓ 166
∓ 168
∓ 170
∓ 172
∓ 174
∓ 176
∓ 178
∓ 180

Figure 17f.

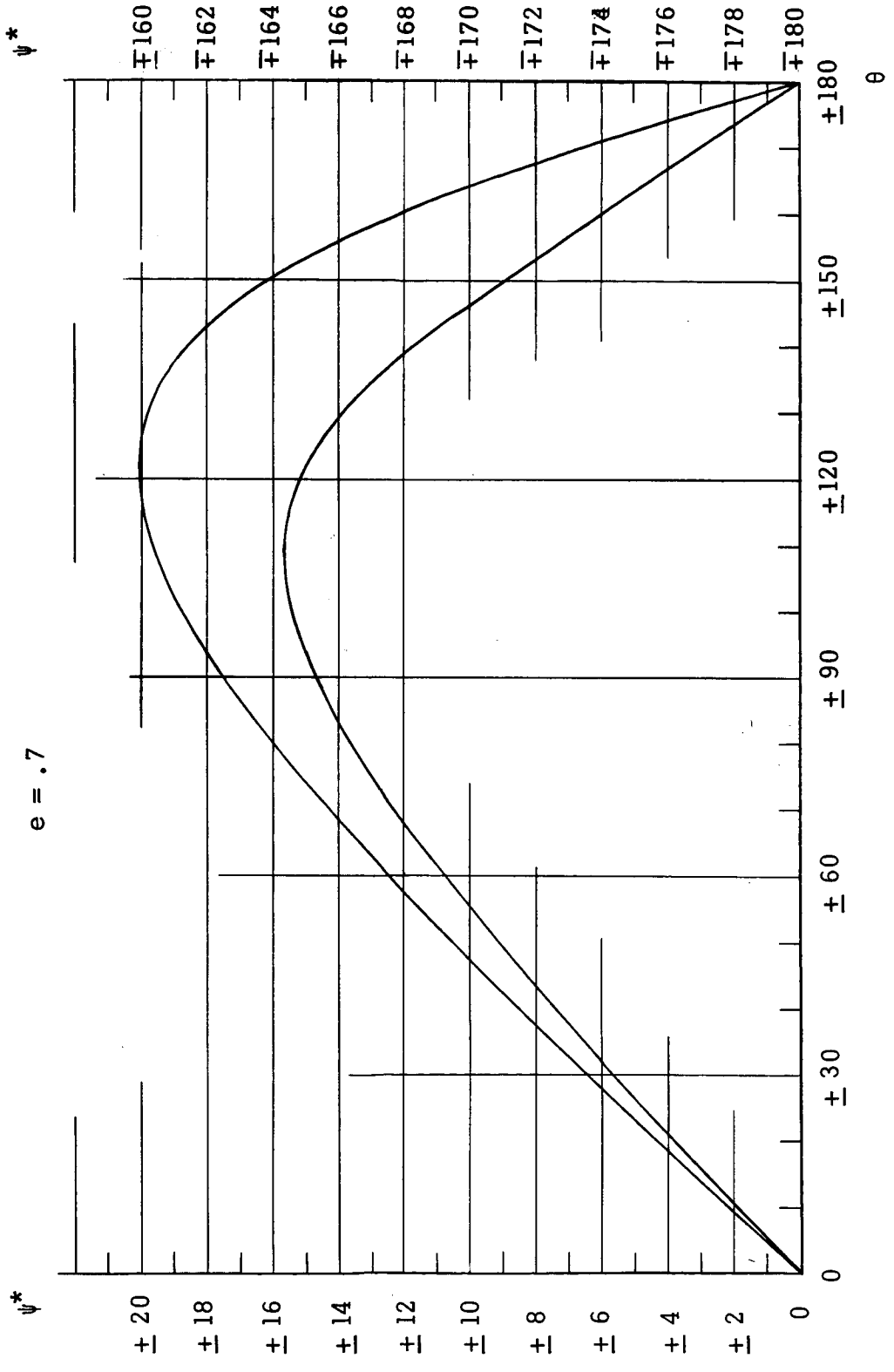
ψ*
ψ*
e = .7
θ
0
± 30
± 60
± 90
± 120
± 150
± 180
0
± 2
± 4
± 6
± 8
± 10
± 12
± 14
± 16
± 18
± 20
∓160
∓162
∓164
∓166
∓168
∓170
∓172
∓174
∓176
∓178
∓180

Figure 17g.

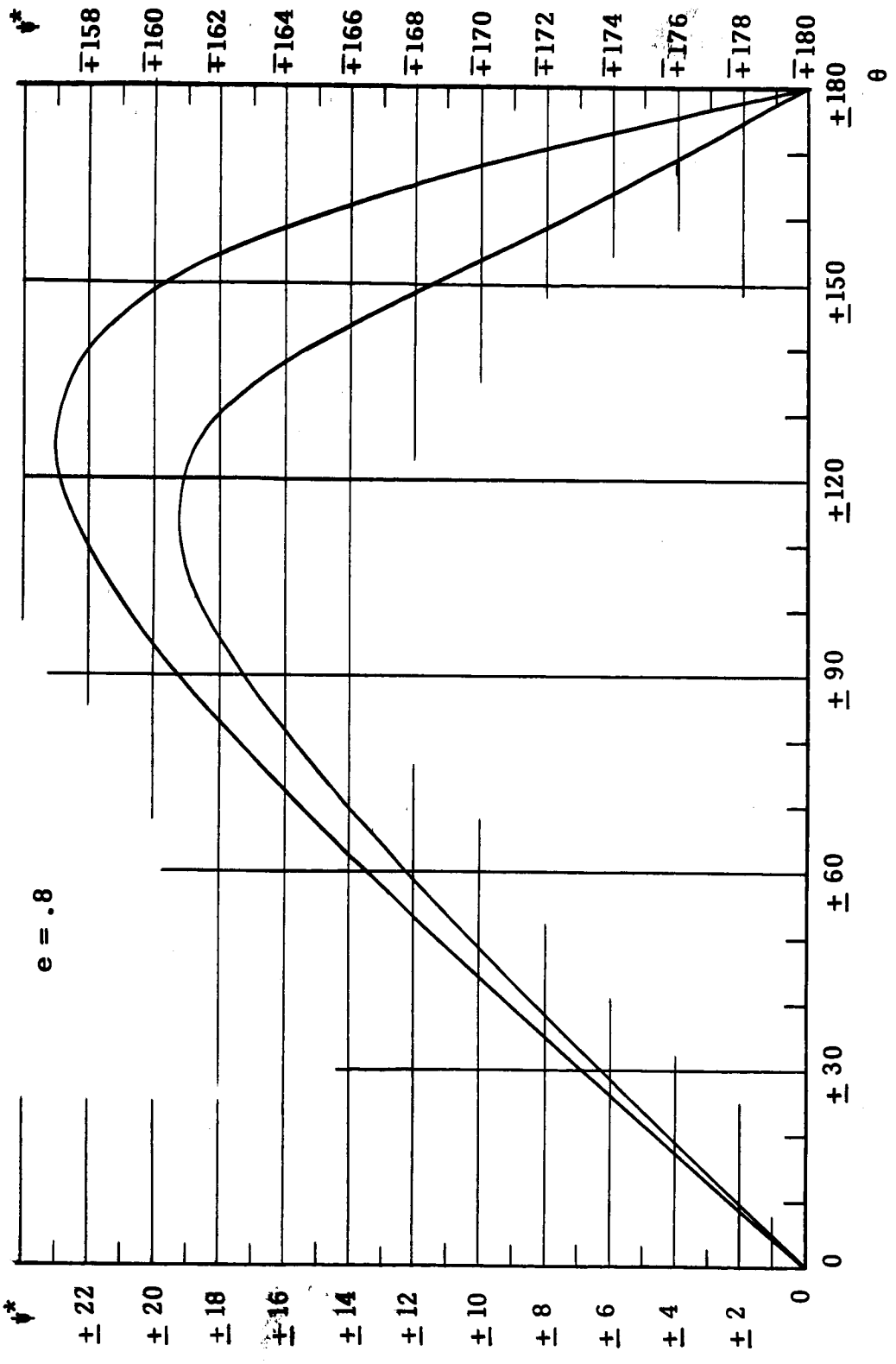
e = .8
θ
0
± 30
± 60
± 90
±120
±150
±180
0
± 2
± 4
± 6
± 8
± 10
± 12
± 14
± 16
± 18
± 20
± 22
∓158
∓160
∓162
∓164
∓166
∓168
∓170
∓172
∓174
∓176
∓178
∓180

Figure 17h.

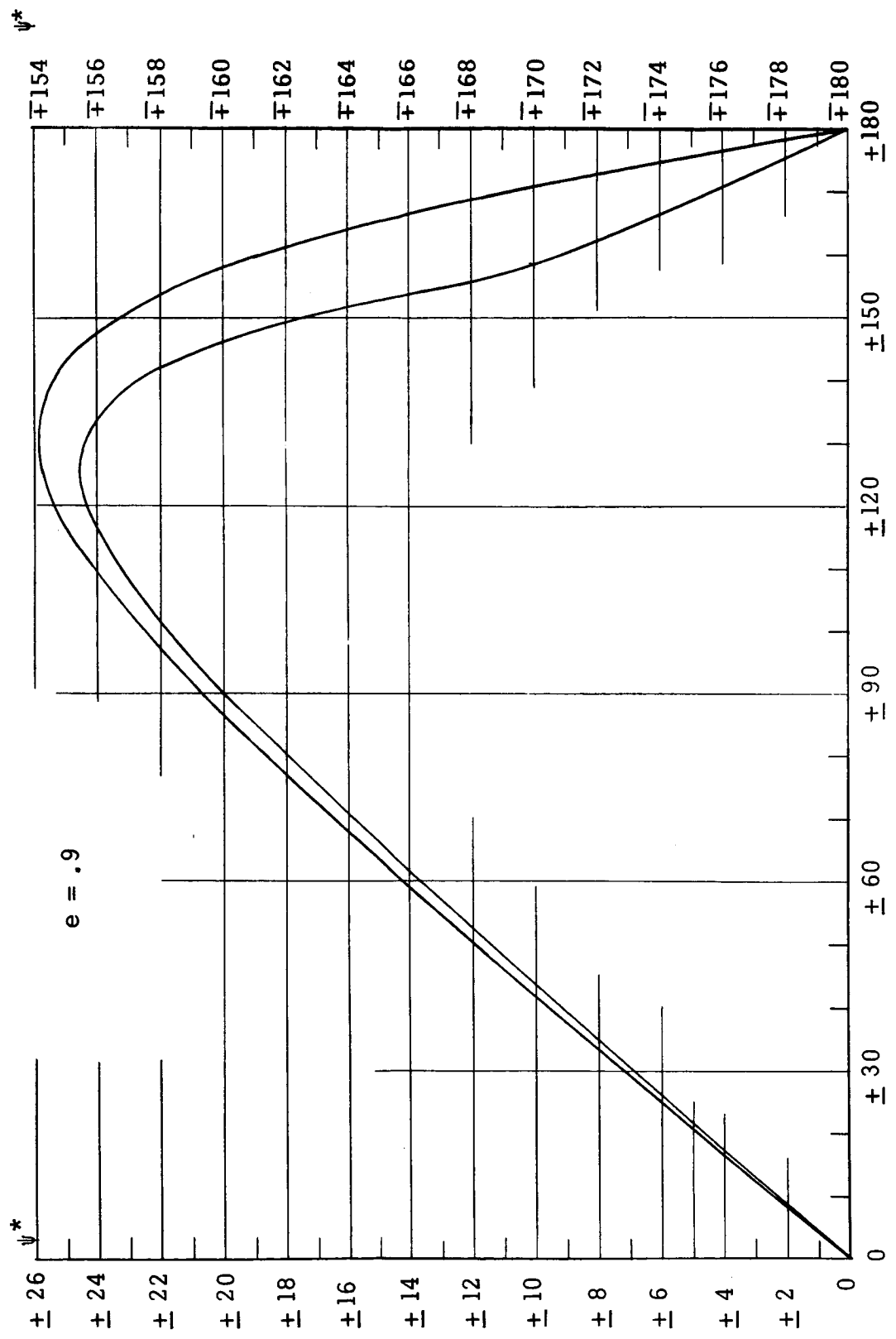
ψ*
∓154
∓156
∓158
∓160
∓162
∓164
∓166
∓168
∓170
∓172
∓174
∓176
∓178
∓180
θ
±150
±120
± 90
± 60
± 30
0
ψ*
± 26
± 24
± 22
± 20
± 18
±16
± 14
± 12
± 10
± 8
± 6
± 4
± 2
0
e = .9

Figure 17i.

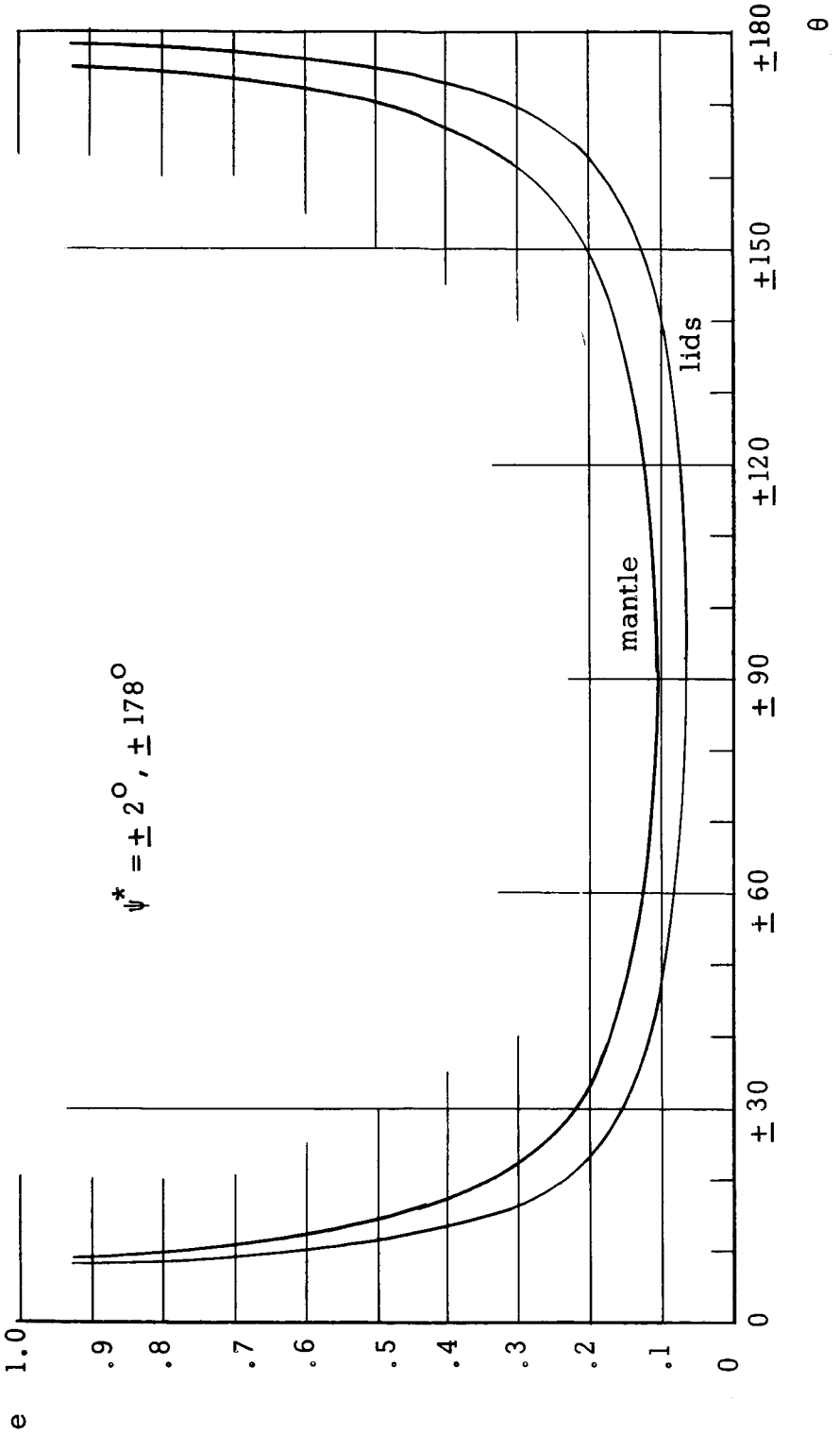

Figure 18a.

Figure 18. Positions and eccentricities which satisfy the necessary condition, for fixed direction of impulse.

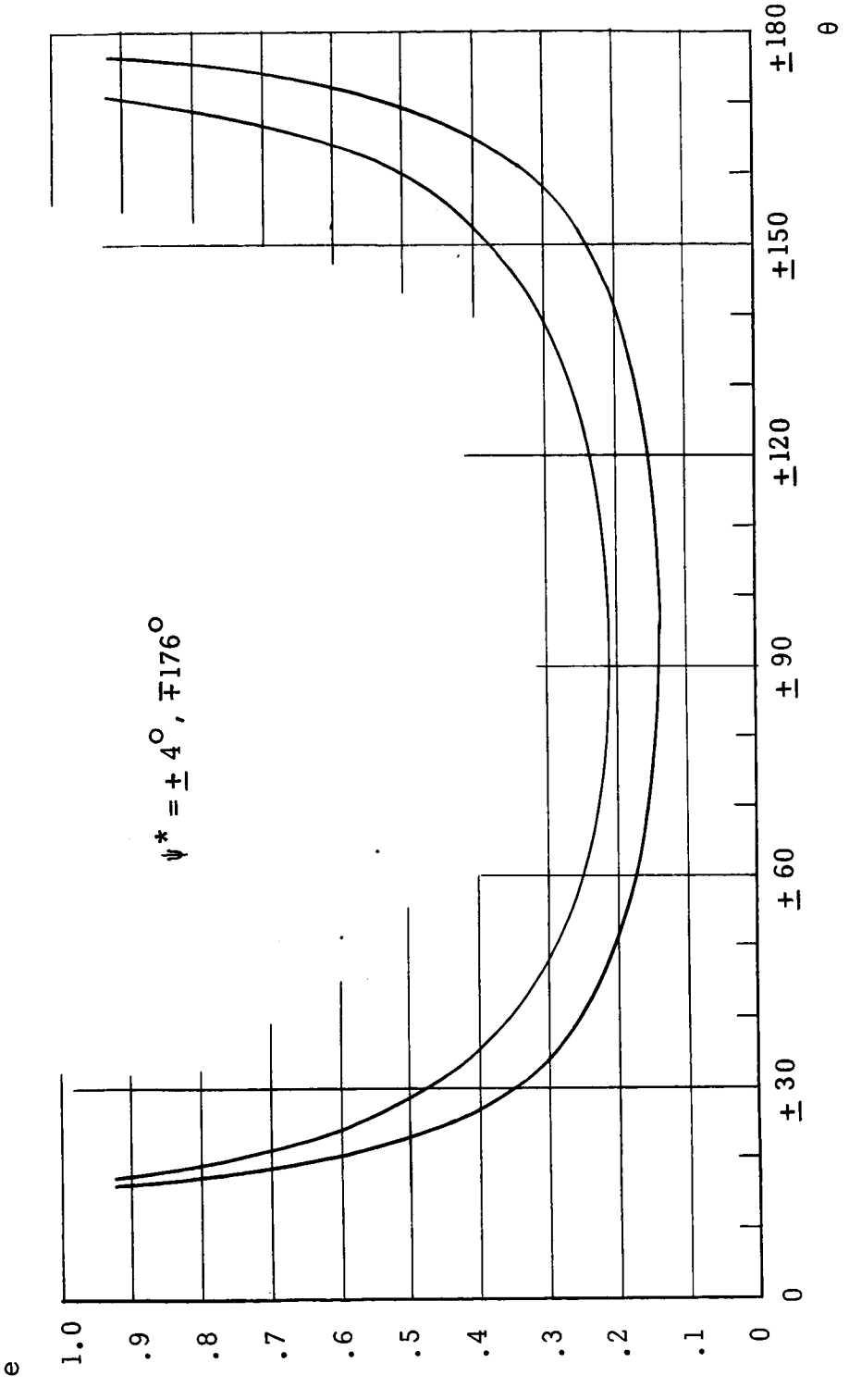

Figure 18b.

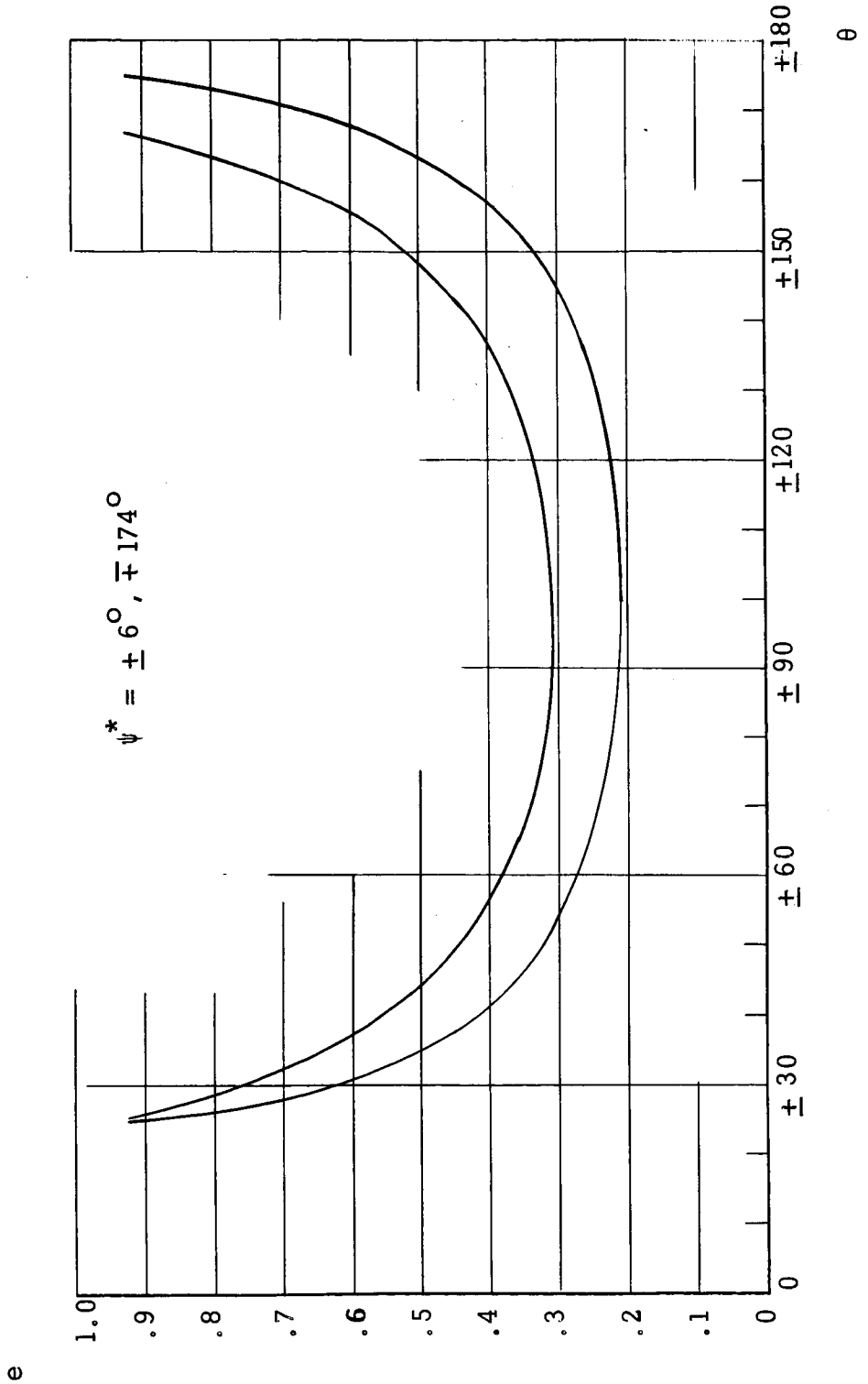

Figure 18c.

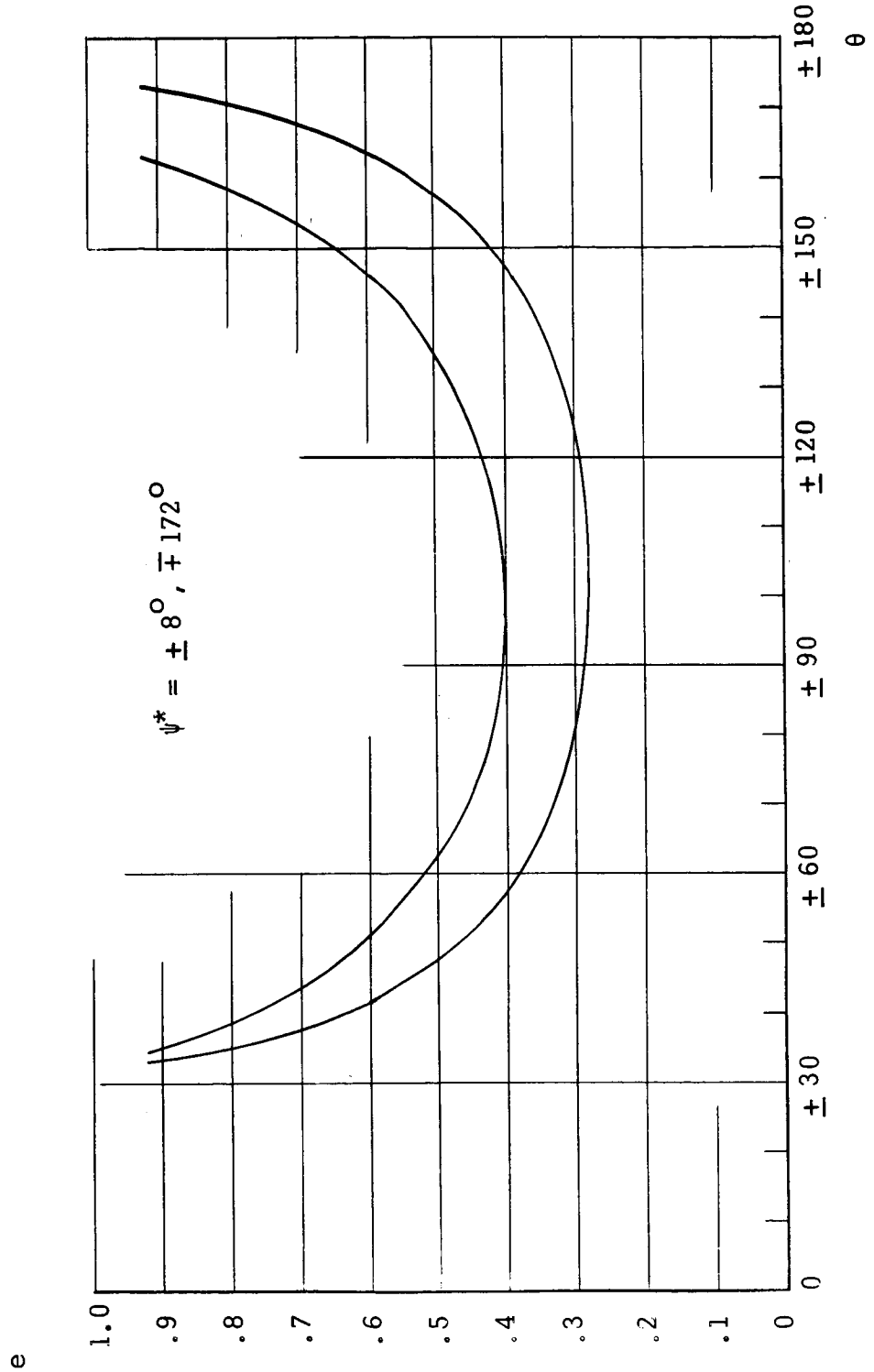

Figure 18d.

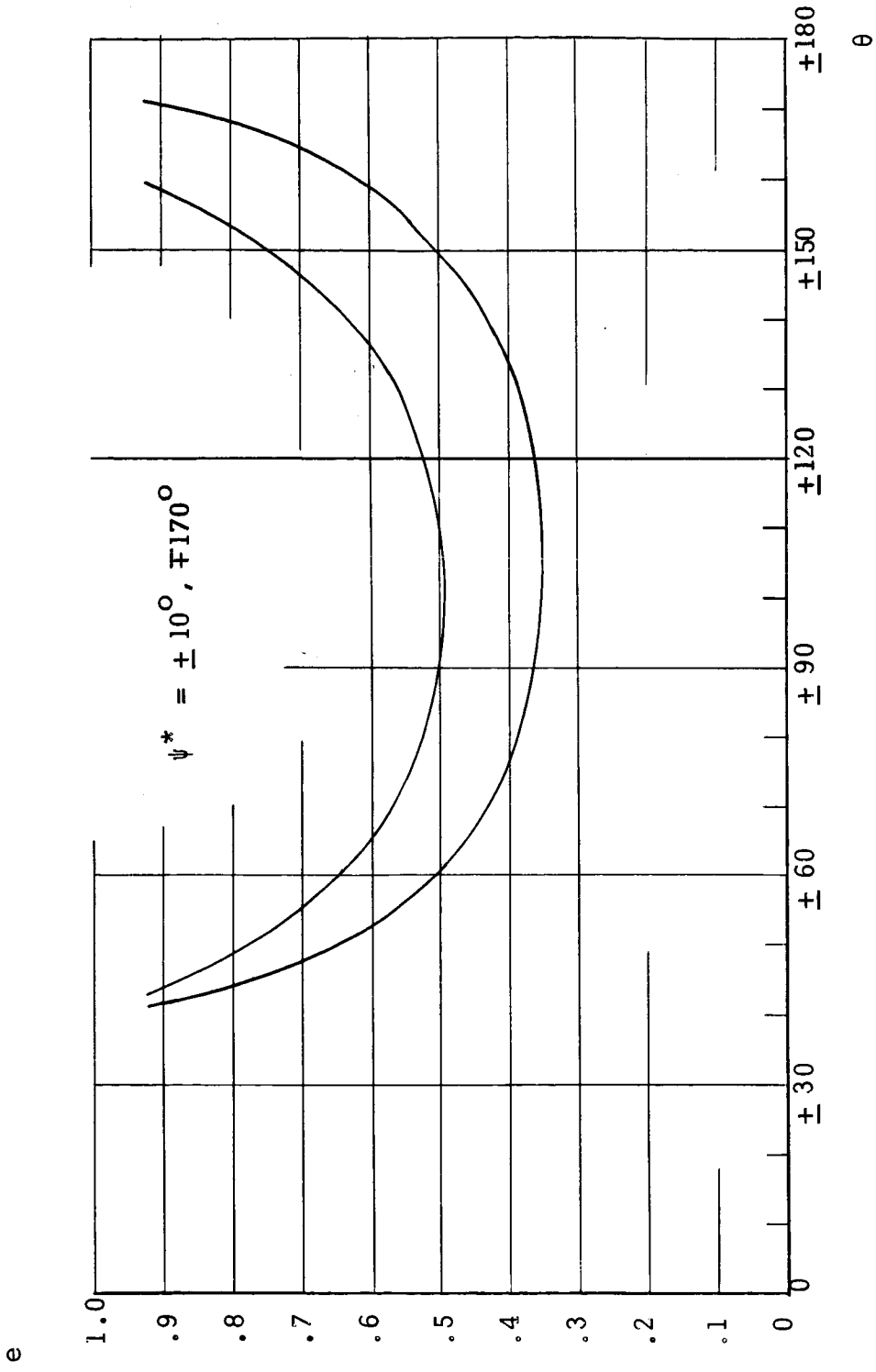

Figure 18e.

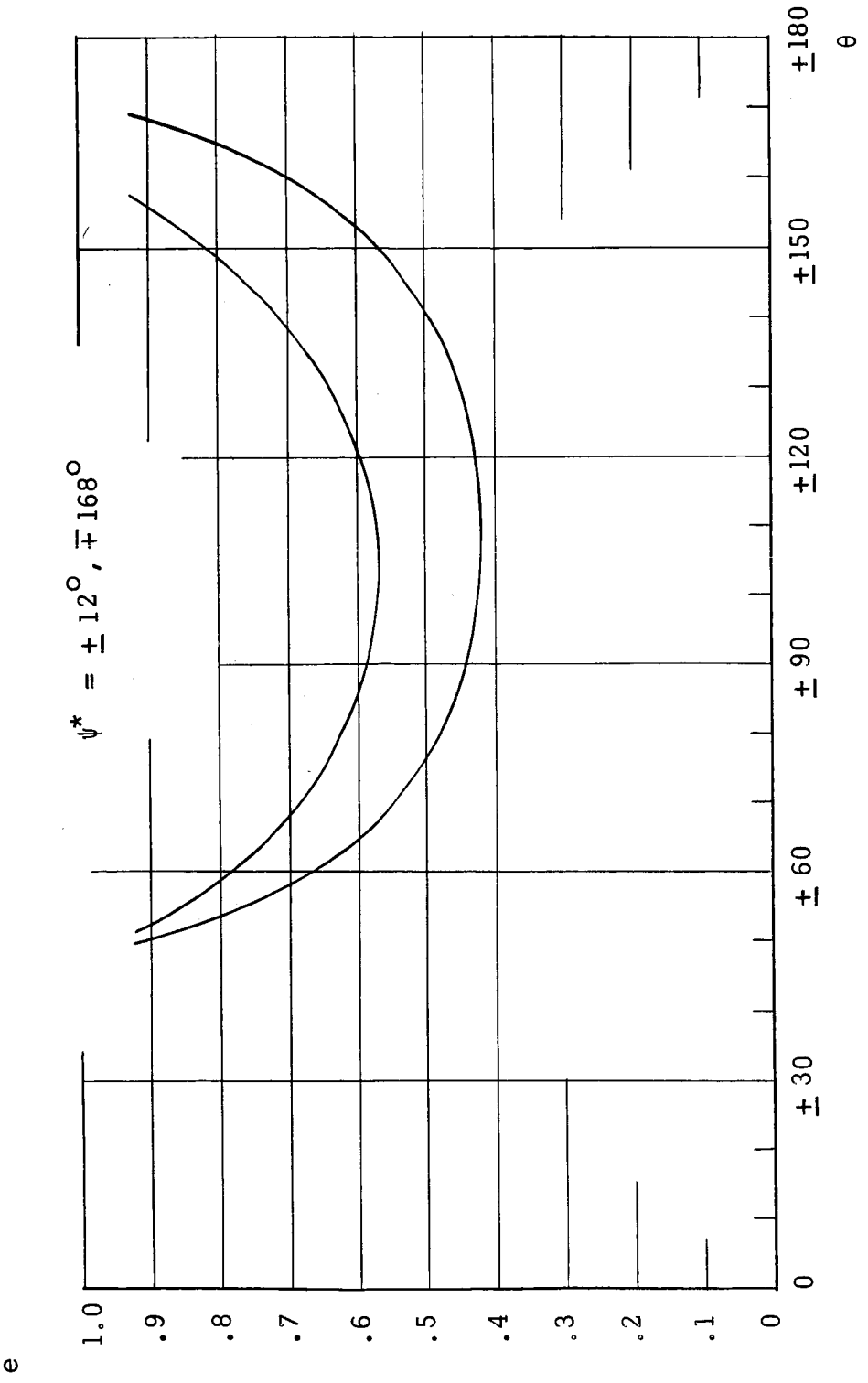

Figure 18f.

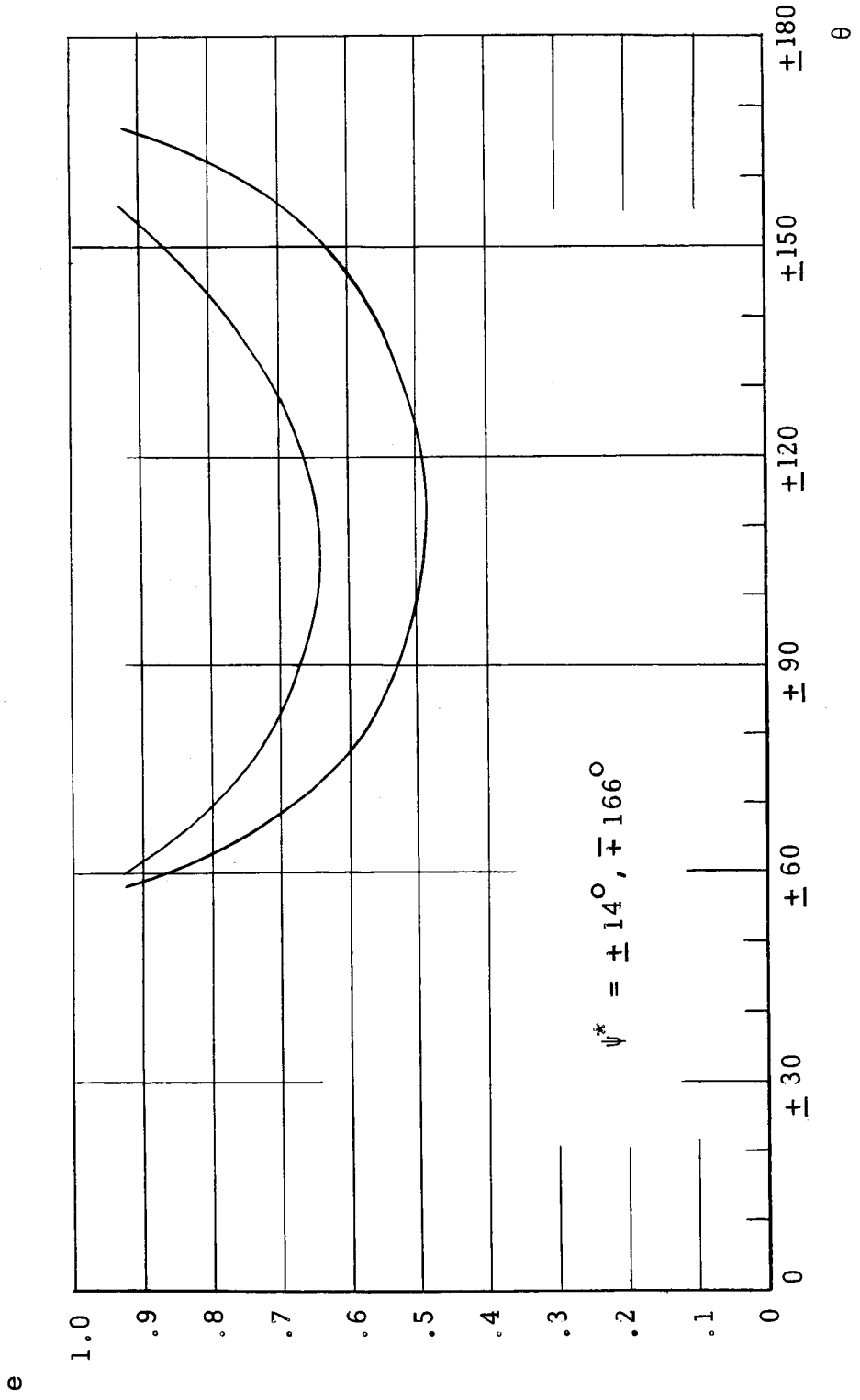

Figure 18g.

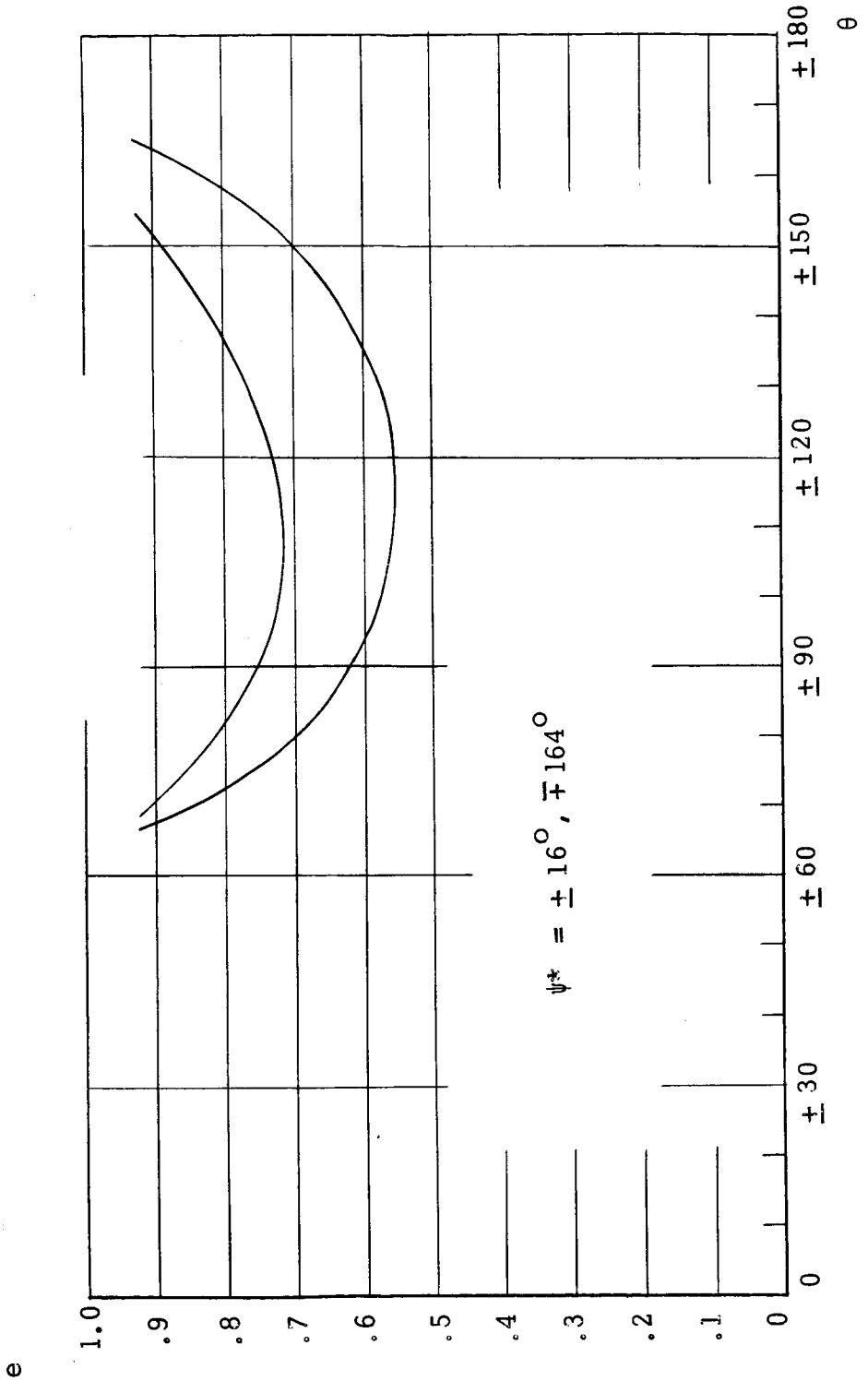

Figure 18h.

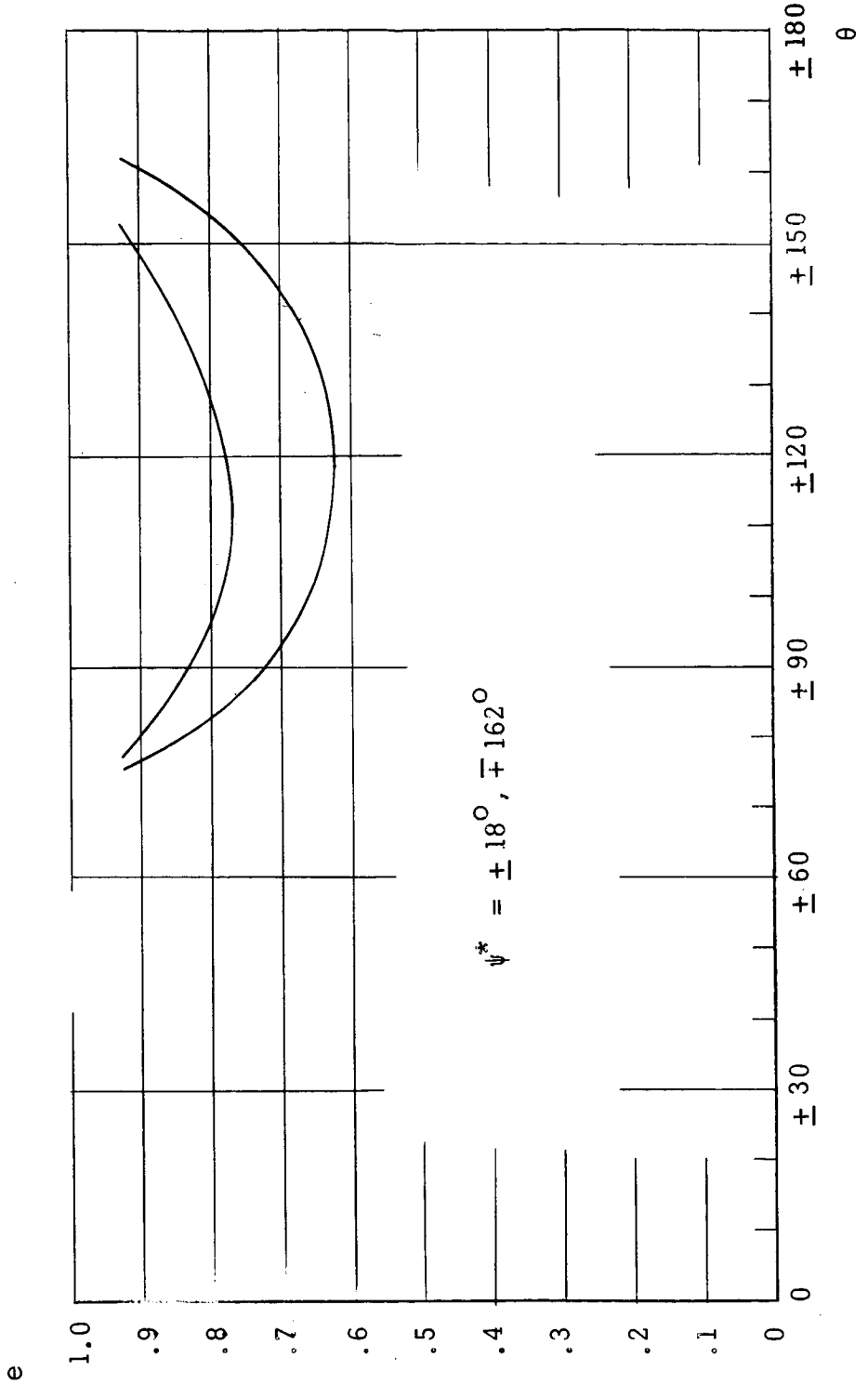

Figure 18i.

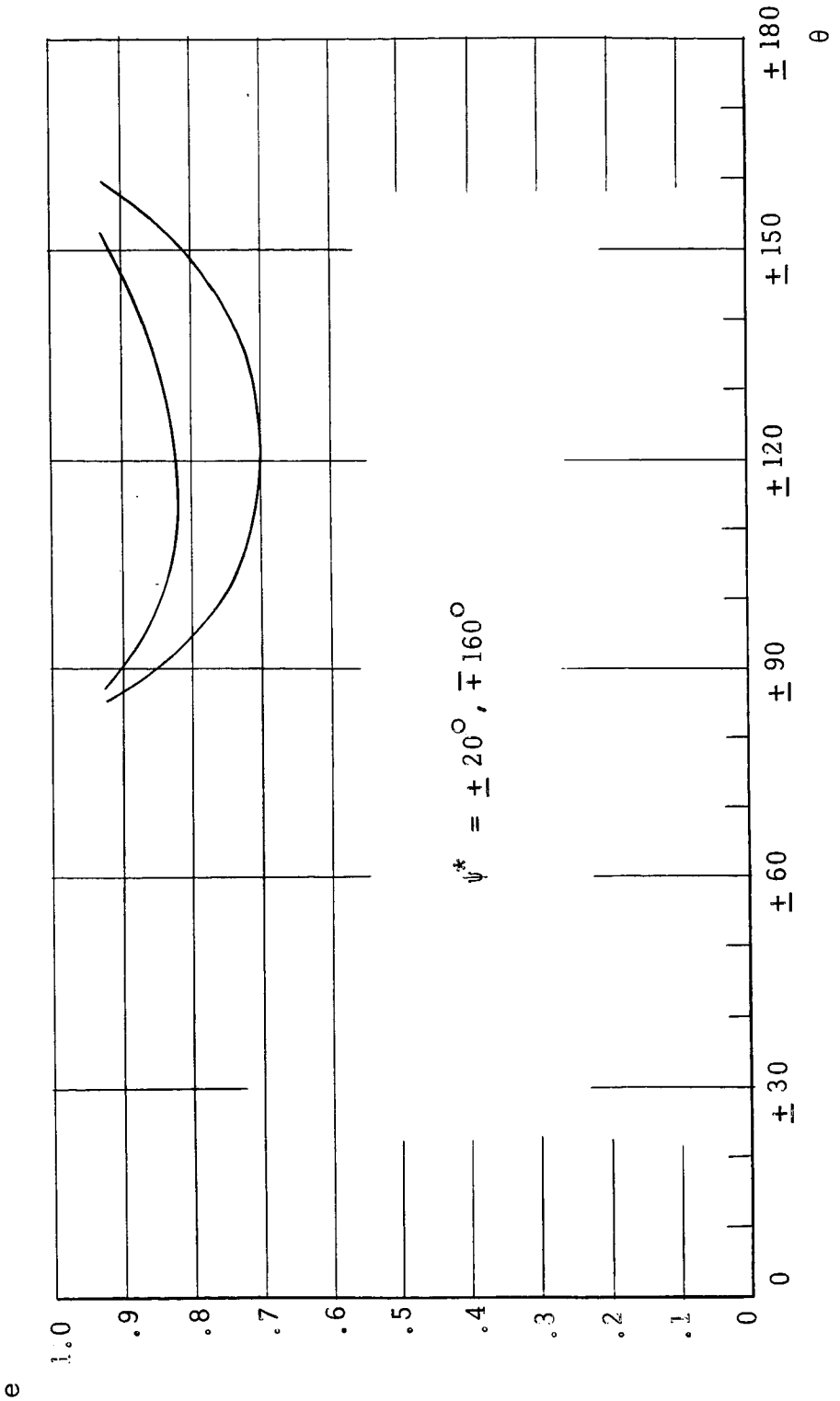

Figure 18j.

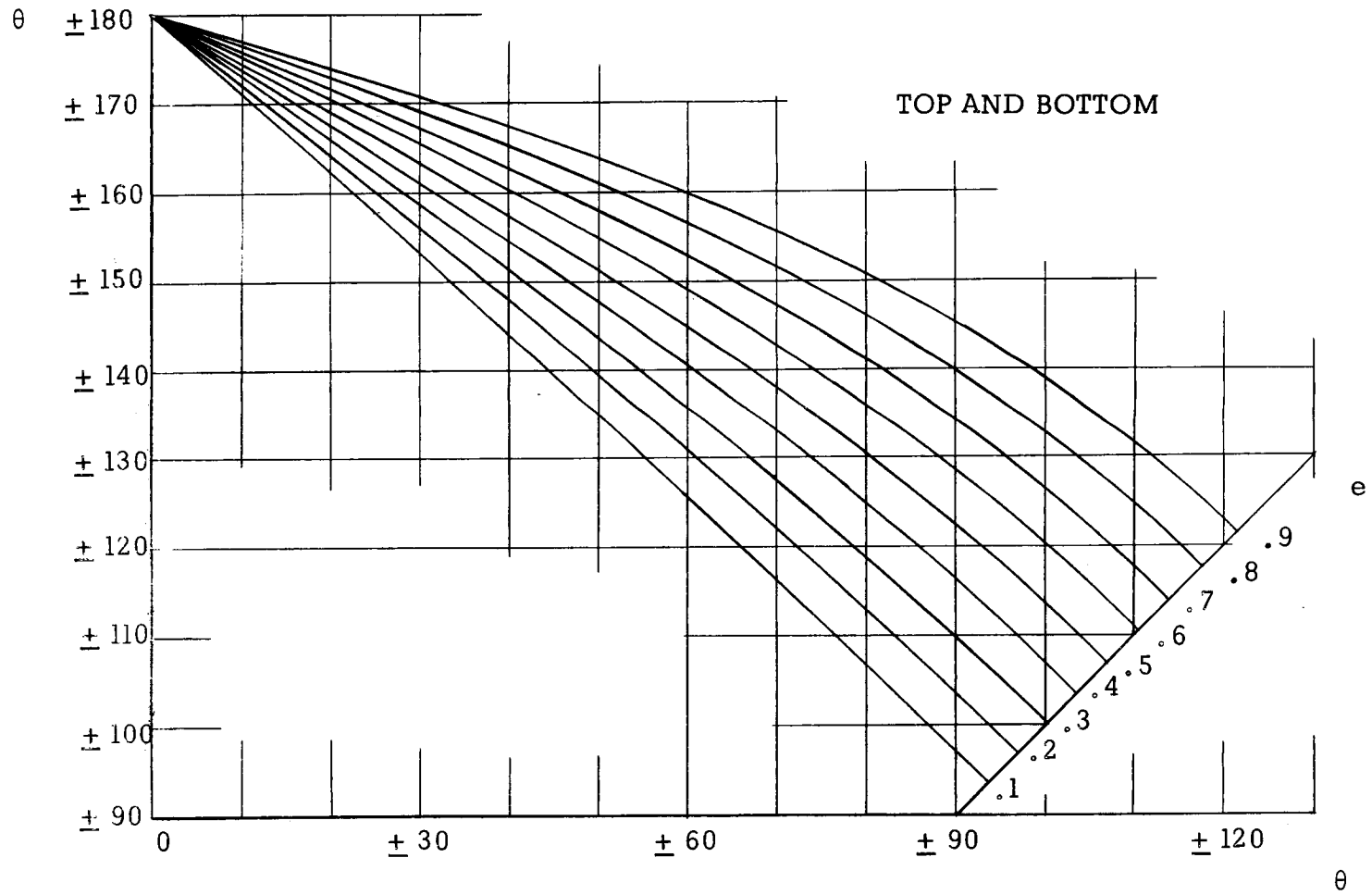

Figure 19. Positions of endpoints of bitangents forming the boundary of the top and bottom developable surfaces.

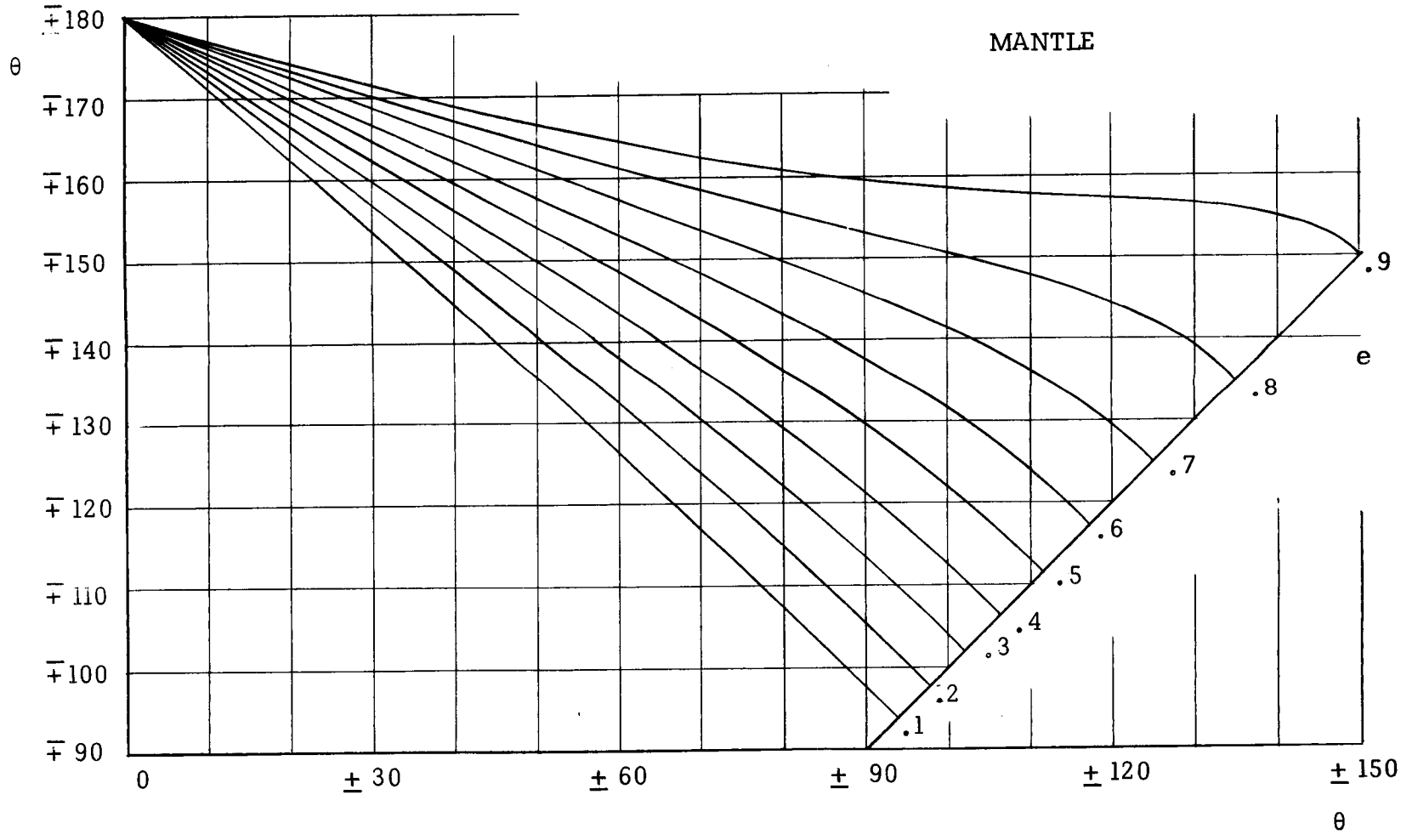

Figure 20. Positions of endpoints of bitangents forming the boundary of the side developable surface.

b) Sample Multiple Impulse Maneuver

In section II g) is discussed the generation of multiple impulse trajectories which are composed of impulses which at all points satisfy the necessary condition and which are joined by corners of only the particular permissible class arising from the bitangents. Here a specific example of such generation is presented.

The characteristic length L of equation (39) is set equal to the value of the length of the major axis of the initial orbit, ℓ_a. The initial orbit is fixed by

$$e_a = .600$$
$$\ell_a = 1.000 \qquad (54)$$

The direction and position of the first impulse is chosen to be

$$\psi_1^* = 10^\circ \quad \text{(constant)}$$
$$\theta_{1,a} = 150^\circ \qquad (55)$$

As can be seen in Figure 21, this impulse is well within the region which satisfies the necessary condition for optimality for sufficiently small impulses.

The equations for the variation of the elements, equations (40), (41), and (43), are integrated numerically using a simple Euler's

technique with increments of the independent variable u from equation (39) taken as .001, and the result is plotted in Figure (21). The arc representing the impulse is followed through the region in which the impulse satisfies the necessary condition until it crosses the boundary and enters the region of forbidden maneuvers. The last point of this arc which still satisfies the necessary condition is the point b on the boundary marked in Figure 21. This marks the termination of the first impulse.

The magnitude of the first impulse is found to be

$$\Delta u_1 = .437 \tag{56}$$

At the termination of the first impulse the orbit is given by

$$e_b = .523$$

$$\ell_b = 2.000 \tag{57}$$

and the position on this new orbit is given by

$$\theta_{1,b} = 80^\circ \tag{58}$$

The rotation of the major axis is found from equation (34) to be

$$\Delta\beta_1 = 70^\circ \tag{59}$$

Since the top boundary line in Figure 21 is violated, the bitangent to be used is a member of the side developable surface. Since the

first impulse is a forward impulse and, therefore, energy is being added to the orbit and ℓ increasing, this boundary is the top boundary of the mantle. Thus, the other end of the bitangent is on the lower boundary of the mantle.

From the corner condition comes the requirement that the next impulse be that represented by the opposite end of this bitangent. From Figure 20, using θ equal to 80 degrees and e equal to .523, one finds the position of the second impulse on the orbit at b as

$$\theta_{2,b} = -138^{\circ} \tag{60}$$

Using θ as - 138 degrees and interpolating between Figures 17e and 17f for e equal to .523, one obtains the direction of the second impulse.

$$\psi_2^* = 172^{\circ} \tag{61}$$

The lower curve is used since the bitangent involved is on the mantle, and the right-hand scale is read since the second impulse is on the lower boundary of the mantle.

The junction between the first and second impulses chosen as described satisfies the corner condition discussed in section II g). The two impulses at the junction point are represented by opposite endpoints of a bitangent which is a member of one of the

developable surfaces of the metric body at the junction point.

The second impulse is started with the position and direction given by equations (60) and (61). Between the end of the first impulse and the beginning of the second impulse the vehicle is simply coasting around the orbit it had at the end of the first impulse. Thus, the orbit at the start of the second impulse is the same as at the end of the first impulse, given by equation (57).

The numerical integration to find the elements of the orbit during the second impulse is performed as before. The arc representing this impulse is shown in Figure 22. This arc crosses the boundary and enters the forbidden region at the point d, marking the termination of the second impulse as dictated by the necessary condition.

At this point the magnitude of the second impulse is found to be

$$(\Delta u_2)_d = .450 \tag{62}$$

The orbit at d is given by

$$e_d = .920$$

$$\ell_d = 1.343 \tag{63}$$

The position on the orbit d at the termination of this impulse is given by

$$\theta_{2,d} = -173^{\circ} \tag{64}$$

The rotation of the major axis during the second impulse is found from equation (34) to be

$$\Delta\beta_2 = 35^{\circ} \tag{65}$$

The total rotation of the major axis during the two impulses is

$$\Delta\beta_{1,2} = 105^{\circ} \tag{66}$$

Using the corner condition as before, one obtains the position and direction of the next impulse as

$$\begin{aligned} \theta_{3,d} &= -24^{\circ} \\ \psi_3^* &= 174^{\circ} \end{aligned} \tag{67}$$

However, as is pointed out in section II g), one maneuver which always competes in the large is the four impulse transfer. From equation (53) the minimum escape impulse from the initial orbit is

$$(\min \Delta u_{esc})_a = .334 \tag{68}$$

The characteristic velocity of the four impulse maneuver at some intermediate ellipse, passed through during the multiple impulse maneuver being generated, is this value plus the minimum escape

impulse from the intermediate ellipse. If for any intermediate orbit the four impulse transfer has a lower characteristic velocity than the characteristic velocity used up to that point in the maneuver being generated, then the multiple impulse maneuver has been defeated by the four impulse maneuver and can be optimal no farther.

Performing this comparison along the path generated, one finds that at the point c the four impulse maneuver overtakes the generated maneuver, and is cheaper from then on. Of course, the four impulse maneuver and the generated maneuver must also be compared between every pair of intermediate points. This proves to be rather simple and no segment of the maneuver a to c can be replaced.

At the point c the magnitude of the second impulse is given by

$$(\Delta u_2)_c = .134 \tag{69}$$

and the minimum escape impulse is

$$(\min \Delta u_{esc})_c = .237 \tag{70}$$

The characteristic velocity of the four impulse maneuver between a and c, (68) plus (70), and the characteristic velocity of the generated multiple impulse maneuver between a and c, (56)

plus (69), are both equal to

$$\Delta u_{a,c} = .571 \tag{71}$$

The orbit at the point c is given by

$$e_c = .654$$
$$\iota_c = 1.683 \tag{72}$$

and the position in the orbit at the termination of the second impulse is

$$\theta_{2,c} = -155.5^{\circ} \tag{73}$$

The rotation of the major axis during this maneuver is

$$\Delta\beta_{1,2} = 87.5^{\circ} \tag{74}$$

In this manner a multiple impulse maneuver has been generated beginning at the orbit a, given by equations (54), and reaching any intermediate orbit on its path up to and including c, given by equations (72). This maneuver everywhere satisfies the necessary condition for optimality, has a junction of two impulses which satisfies the corner condition, and is cheaper than the competing four impulse maneuver.

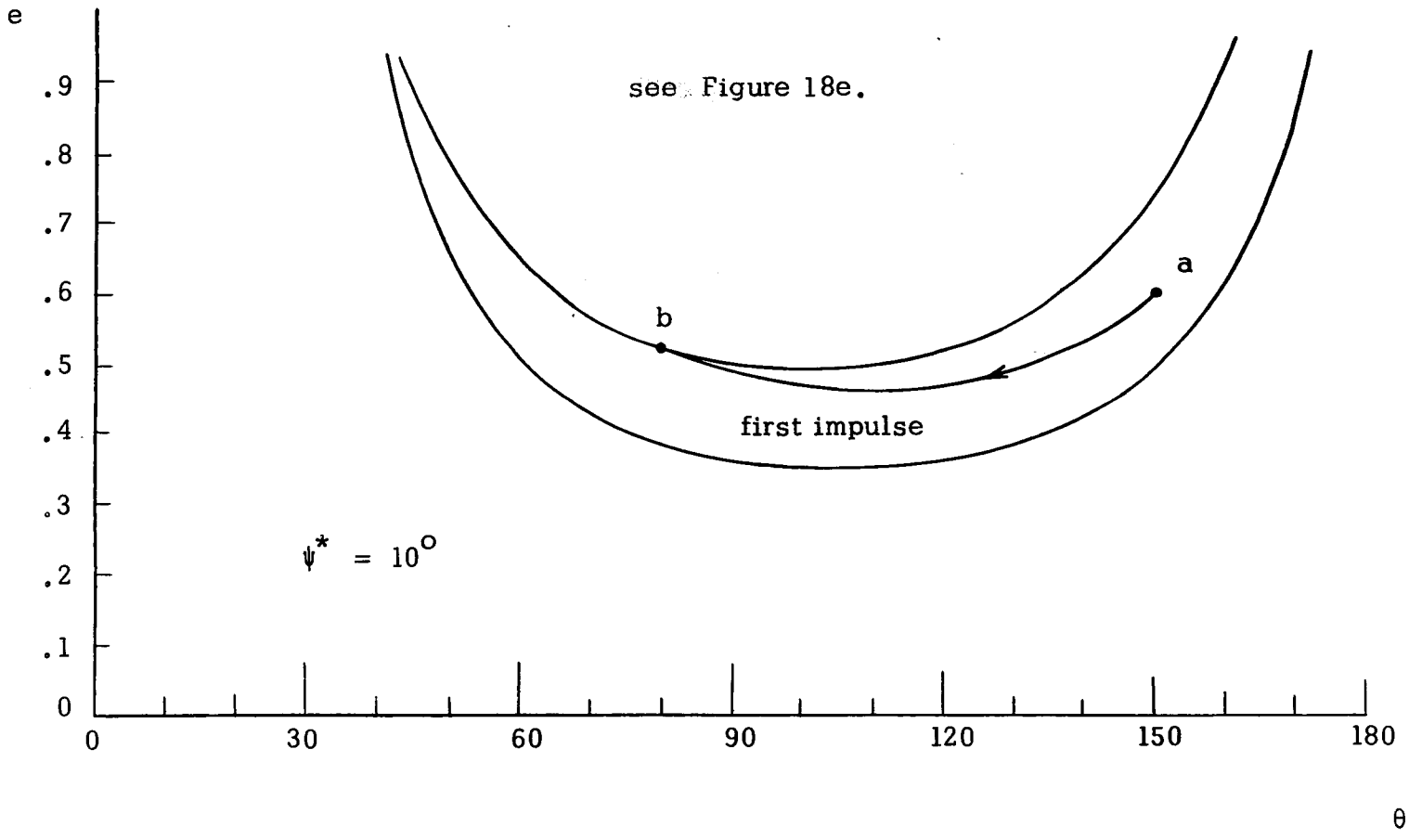

Figure 21. First impulse of sample multiple impulse generation.

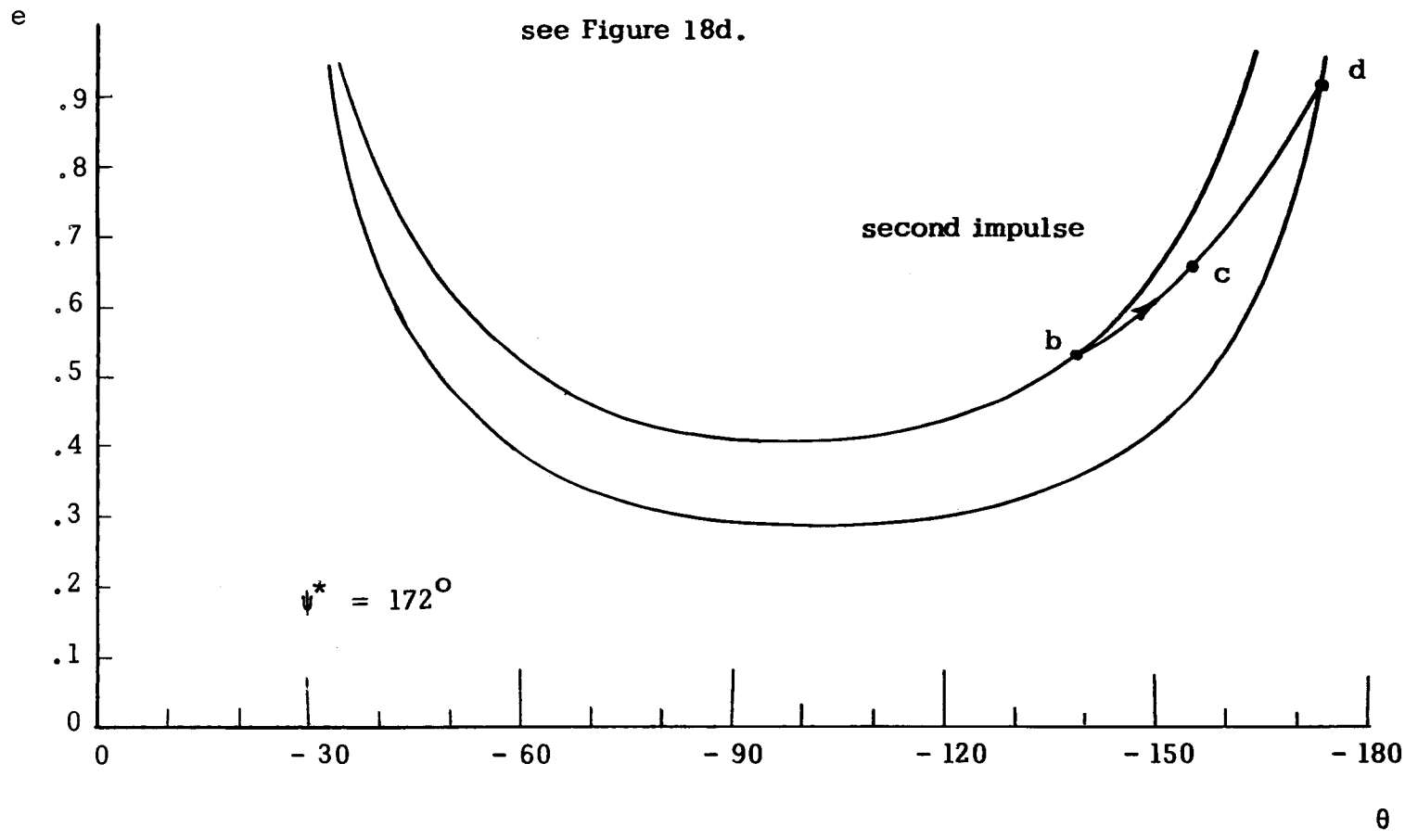

Figure 22. Second impulse of sample multiple impulse generation.

c) Conclusion

This study produces a necessary condition which must be satisfied by any impulsive coplanar maneuver in order that it be an optimal maneuver, and a corner condition which must be satisfied when connecting impulses in order that the resulting multiple impulse maneuver be optimal. Since any continuous thrust maneuver can be made up of an infinite number of infinitesimal impulses all of which must satisfy the necessary condition for optimality and must be joined in agreement with the corner condition, these results apply to all optimal paths, both impulsive and continuous types.

The necessary condition is that at every point of an impulse its direction and position must be such that it is represented by a point in the convex portion of the local metric body. The corner condition is that if two distinctly different impulses are joined, they must be represented at the junction by opposite endpoints of a bitangent member of one of the developable surfaces covering a concave portion of the local metric body.

It is found that the direction of the impulses which satisfy the necessary condition must always lie between the local horizontal and the tangential directions. In fact, it is found that ψ^*, or $\min |\psi^* \pm 180^\circ|$, is never larger than .53 of the magnitude of γ, the local flight path angle. For a given eccentricity e and position

θ, the spread of allowable ψ^*/γ is approximately .1 to .2, though it varies somewhat. This is in agreement with the excellent work of Marchal[11], which follows and extends the pioneering work of Contensou[4]. Marchal obtains a bound on the spread of the allowable ψ^*, and through asymptotic expansions gets approximate expressions for the requirements for joining two impulses. Moyer[17] also finds that a single impulse must be directed between the horizontal and the tangential directions. Moyer uses a method outlined by Breakwell[18] which is based, in turn, on Contensou's paper. Moyer's results are entirely numerical.

It should be pointed out that this study in no way restricts the sense of circulation of the orbits considered. The results presented are for orbits with the same sense of circulation, however, the solution for a transfer between orbits with opposite circulation is obvious. Since such a transfer involves passing through a state of zero angular momentum, the solution will always be Marchal's four impulse transfer.

In this present study a method is set forth for generating multiple impulse maneuvers which satisfy the necessary condition and corner condition of this analysis. These multiple impulse maneuvers are checked against Marchal's four impulse transfer between orbits[11]. The multiple impulse trajectory is terminated when the four impulse maneuver shows it to be nonoptimal. In this

manner a map of such multiple impulse arcs throughout the configuration space can be produced. This method for generating multiple impulse maneuvers also leads to the continuous thrust optimals as is discussed below. This intriguing area is not fully covered here, but is left for future analysis.

This study indicates several areas which are of interest for future investigations. The mapping of configuration space with multiple impulse arcs generated from this necessary condition and joined subject to the corner condition may lead to a deeper insight of this optimization problem, and to better generalizations of the solutions.

It also appears possible to obtain a similarity law expressing the necessary condition in terms of the local flight path angle. At this time, unfortunately, only an empirical or approximate law seems feasible.

This study extends from e equal to zero to e equal to .9, though the results can be extrapolated a short distance farther. Further study should be made of the metric body and the resulting necessary and corner conditions in the vicinity of e equal to one. Some work has been done on this [11,17,18] and it appears that the situation changes considerably for almost parabolic orbits. Using other methods, these investigators find for e greater than .925 there are positions on the orbit from which no possibly optimal maneuvers

are available.

In addition, there is the interesting possibility of finding a bitangent member of a developable surface of the metric body each of the endpoints of which indicate a switch to the other after an infinitesimal impulse. This would be the chattering entry to an optimal intermediate thrust trajectory discussed by Robbins[7], and currently being investigated by several others[10]. The effect of an intermediate, or continuous, thrust program is simulated by an infinite number of infinitesimal impulses, separated only by infinitesimal coasting arcs. Therefore, the positions in the orbit, given by the values of θ at each end of the bitangent, would have to be separated only infinitesimally. This dictates that such bitangents may be found only along the 45 degree line in Figure 19.

Finally, this same technique can be extended to the same problem without the coplanar restriction. The noncoplanar problem requires a five dimensional configuration space, with three degrees of freedom for the infinitesimal impulse which generates the metric body. Thus, the metric body is a three dimensional hypersurface imbedded in a five dimensional space. This metric body will be rendered convex by three dimensional hyperplanes generating the developable surfaces which cover the concave portions of the metric body. The contributions of visualization and intuition are reduced to nearly negligible quantities. The tremendously increased complexity

of the noncoplanar problem points out the reason it has been only briefly considered up until now. This is also the reason this present analysis is strictly coplanar. However, the possibility of such an extension cannot be neglected.

Bibliography

1. Hohmann, W., "Die Erreichbarkeit der Himmelskörper" R. Oldenbourg, Munich, 1925. English translation: "The Attainability of Heavenly Bodies" NASA Tech. Translation F-44 (1960).

2. Busemann, Adolf, "Minimalprobleme der Luft- und Raumfahrt" The 1965 Ludwig Prandtl Lecture delivered April 23, 1965 in Vienna. Published in Zeitschrift fur Flugwissenschaften, 13, Heft 11, pp.401 - 411, November, 1965.

3. Vinh, Nguyen Xuan, "Geometrical Studies of Orbital Transfer Problems" Ph.D. Thesis, Department of Aerospace Engineering Sciences, University of Colorado, December, 1964.

4. Contensou, P., "Etude théorique des trajectoires optimales dans un champ de gravitation. Application au cas d'un centre d'attraction unique" Astronautica Acta, Vol. 8, pp. 134 - 150, 1962.

5. Lawden, D.F., Optimal Trajectories for Space Navigation, Butterworths, London, 1963.

6. Kopp, R.E., and Moyer, H. Gardner, "Necessary Conditions for Singular Extremals" AIAA Journal, Vol. 3, No. 8, pp. 1439 - 1444, August, 1965.

7. Robbins, H.M., "Optimality of Intermediate-Thrust Arcs of Rocket Trajectories" AIAA Journal, Vol. 3, No. 6, pp. 1094 - 1098, June, 1965.

8. Pines, Samuel, "Constants of the Motion for Optimum Thrust Trajectories in a Central Force Field" AIAA Journal, Vol. 2, No. 11, pp. 2010 - 2014, November, 1964.

9. Handelsman, Morris, "Optimal Free-Space Fixed-Thrust Trajectories Using Impulsive Trajectories as Starting Iteratives" AIAA Journal, Vol. 4, No. 6, pp. 1077 - 1082, June, 1966.

10. Edelbaum, T.N., "How Many Impulses?" AIAA 3rd Aerospace Sciences Meeting, Paper No. 66-7, January, 1966.

11. Marchal, C., "Transferts optimaux entre orbites elliptiques coplanaires (Durée Indifférente)" Astronautica Acta Vol. 11, No. 6, pp. 432 - 445, 1965.

12. Busemann, A., Vinh, N.X., and Culp, R.D., "Geometric Constraints of the Disorbit Problem," University of Colorado College of Engineering, Department of Aerospace Engineering Sciences, Publication 66(AES) - 1, January, 1966.

13. Battin, Richard H., Astronautical Guidance, McGraw-Hill, pp. 111 - 112, 1964.

14. Vinh, N.X., "A Property of Cotangential Elliptical Transfer Orbits" AIAA Journal, Vol. 2, No. 10, pp. 1841 - 1844, October, 1964.

15. Ting, Lu, "Optimum Orbital Transfer by Several Impulses" Astronautica Acta Vol. VI, Fasc. 5, pp. 256 - 265, 1960.

16. Barrar, Richard B., "An Analytical Proof that the Hohmann-Type Transfer is the True Minimum Two-Impulse Transfer" Astronautica Acta Vol. IX, Fasc. 1, pp. 1 - 11, 1963.

17. Moyer, H. Gardner, "Necessary Conditions for Optimal Single Impulse Transfer" AIAA 3rd Aerospace Sciences Meeting, Paper No. 66 - 93, January, 1966.

18. Breakwell, John V., "Minimum Impulse Transfer" AIAA Progress in Astronautics and Aeronautics: Celestial Mechanics and Astrodynamics, Vol. 14, edit. V.G. Szebehely, Academic Press, New York, pp. 583 - 589, 1964.

19. Robbins, Howard M., "An Analytical Study of the Impulsive Approximation" AIAA 3rd Aerospace Sciences Meeting, Paper No. 66 - 12, January, 1966.